Models for compressive strength estimation through non-destructive testing of highly self-compacting concrete containing recycled concrete aggregate and slag-based binder

Víctor Revilla-Cuesta [a], Marta Skaf [b,*], Roberto Serrano-López [a], Vanesa Ortega-López [a]

[a] Department of Civil Engineering, University of Burgos, EPS. Calle Villadiego s/n, 09001 Burgos, Spain
[b] Department of Construction, University of Burgos, EPS, Calle Villadiego s/n, 09001 Burgos, Spain

HIGHLIGHTS

- 24 Highly SCC mixes with high contents of Recycled Concrete Aggregate (RCA)
- 2592 Hammer rebound index and 864 UPV analysis performed.
- Conventional models invalid for compressive strength estimations of RCA SCC.
- Non-destructive testing suitable to estimate strength regardless of SCC composition.
- Safe and precise models developed through rebound index and UPV for SCC.

GRAPHICAL ABSTRACT
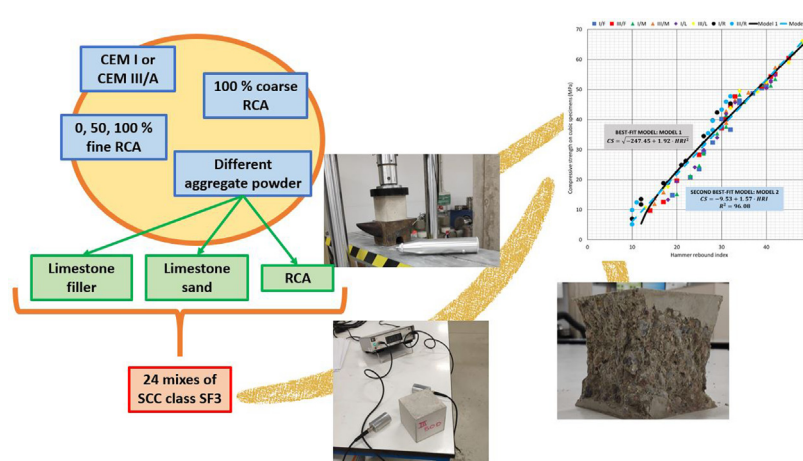
ABSTRACT

Indirect estimation of compressive strength through non-destructive testing is key to monitoring the strength of structural concretes used in construction and rehabilitation works. However, no models are available to perform this estimation in highly Self-Compacting Concrete (SCC) with Recycled Concrete Aggregate (RCA). To fill this gap, two indirect measures were tested in this paper, the hammer rebound index and Ultrasonic Pulse Velocity (UPV), to predict the compressive strength of highly SCC. To do so, 24 SCC mixes were developed with different aggregate powders, binders, such as Ground Granulated Blast Furnace Slag (GGBFS), and contents of fine RCA. Compressive strength, and both indirect measures of all mixtures were determined at 1, 7, 28, and 90 days. The development of specific models for highly SCC responded to the inappropriateness of conventional models that are not adapted to its high fines content. Modelling as a function of either UPV or the hammer rebound index yielded accurate predictions, although the UPV model proved more sensitive to compositional changes and presented higher uncertainty. The best predictions were modelled by combining both indirect measures. The models provided safe and accurate indirect estimations of the compressive strength of high flowability SCC in real structures.

© 2021 The Authors. Published by Elsevier Ltd. This is an open access article under the CC BY-NC-ND license (http://creativecommons.org/licenses/by-nc-nd/4.0/).

1. Introduction

Traditionally, non-destructive tests have been used to estimate the compressive strength of concrete [1] in rehabilitation works [2], and for the estimation and monitoring of concrete strength during construction and throughout the lifecycle of the structure [3]. The oldest and the most common methods are the so-called indirect measures: the hammer rebound index, which is based on the surface hardness of the concrete [4], and Ultrasonic Pulse Velocity (UPV) analysis, which depends on the microstructure of the material [5]. Although the use of such semi-destructive methods as penetration resistance [6] and core tests [7] are increasingly widespread, indirect measures are still very useful on site, due to their greater simplicity and quicker execution.

The hammer rebound index test was developed in the 1940s and has been widely used ever since, because of its low cost and ease of use [8]. This test only requires a Schmidt rebound hammer, whose operation is shown in Fig. 1 [9]. When the hammer is moved towards the plunger, which has been previously placed in contact with a concrete surface, preferably at a right angle, a spring attached to the plunger is simultaneously tensed. The energy of the spring is released at the end of the plunger and a calibrated weight is pushed upwards. The distance this mass is displaced, dependent upon the recoil energy of the spring, represents the hammer rebound index value [10]. The validity of this method for the estimation of compressive strength was first demonstrated over half a century ago [11]. Nevertheless it has since been noted that its results will depend on the aggregate properties [4] and their natural source [12], so that its validation will therefore be dependent on statistical models [1].

UPV analysis also emerged in the 1950s [13], although its main advances occurred at the end of the century [14]. UPV is measured by an ultrasonic device, which determines the time (μs) that an ultrasonic signal at a frequency of 1 kHz takes to reach the receiving transducer, from the transmitting transducer [15]. The direct method of performing this measurement is the most common, in which the two transducers are positioned opposite each other (Fig. 2). Both the propagation of internal damage within concrete [16], and its porosity [17] can be evaluated with the UPV test. In addition, it is highly conditioned by the stiffness of the material, so it correlates with the compressive strength and the modulus of elasticity of the concrete [18]. The statistical adjustment of the model is also essential for accurate and safe use [5].
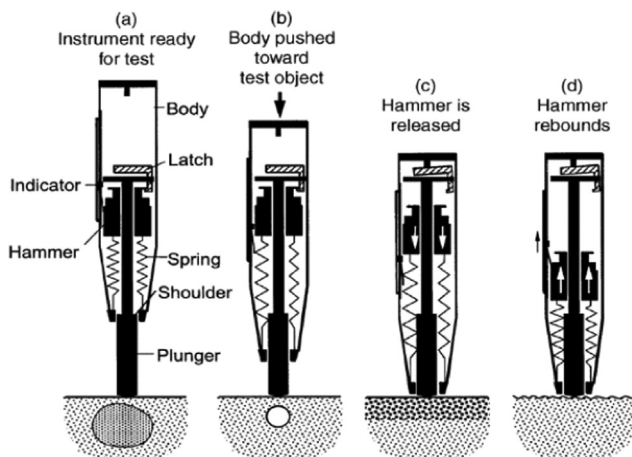
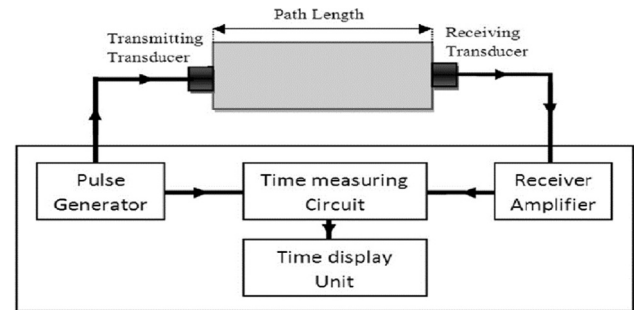**Fig. 1.** Operation of the Schmidt rebound hammer [9].

Fig. 2. UPV device set up for direct measurements [15].

Even though these indirect measures have long been employed, their progress in relation to their use and application in construction has been remarkable since 2000 [19]. Some new trends in this field include their successful use at evaluating the compressive strength of concrete at early ages [20,21], to study the spatial variability of concrete strength [22,23], especially in beams [24], and high-precision detection of micro-cracking within the damaged concrete [2,25], especially with UPV analysis [26]. In addition, there is also a field of research regarding their applicability in concretes made with alternative materials [27,28], and in non-conventional concretes, such as high performance fiber-reinforced concrete [29] and Self-Compacting Concrete (SCC) [30].

Among the new trends in concretes with special applications, SCC is perhaps the most prominent nowadays [31], due to its high flowability in the fresh state, which facilitates placement without vibration [32]. On the other hand, the use of wastes for the production of concrete, including SCC [33], has also been increasing over recent years, as a sustainability improvement strategy within the construction sector [34]. Among the different residues that can be recovered as aggregate for concrete production, such as bricks [35], siderurgic slags [36], and construction and demolition waste [37], Recycled Concrete Aggregate (RCA) stands out [38], due to its mechanical properties [39].

The results of the literature [40], backed up by our own past experience [41], have confirmed that the use of coarse RCA, compared to fine RCA, results in a lesser decrease in the compressive strength of concrete. The few studies on the non-destructive testing of concretes containing RCA have therefore generally been focused on the validity of concrete manufactured with only coarse RCA. In this regard, a relevant conclusion is that the addition of coarse RCA alters the standard benchmarking of indirect measurements and their relationships with compressive strength [42,43]. Nevertheless, they have successfully predicted the behavior of the concrete manufactured with this waste even at 1 day [21], despite the fact that the addition of RCA sometimes delays the development of concrete strength [41]. Finally, it has also been stated that the joint use of two non-destructive methods provides greater security for the estimation of the strength of concrete containing coarse RCA [44], due to the variability of the properties of this recycled aggregate [45]. It is especially significant that the validation of non-destructive testing in concrete manufactured with fine RCA is practically non-existent, as the nature of the finest aggregate fractions affects the accuracy of the concrete strength estimation through indirect measurements [43]. One study concluded that the UPV values were lower when the fine fraction of RCA was used, compared to concrete manufactured with natural aggregates [46], and another one found that linear equations were suitable to predict the compressive strength [47], although it was not checked whether other models provided a more precise fit.

SCC is characterized by a large content of fines and water [48] and therefore a large proportion of cement paste [32] to achieve

proper flowability. The accuracy of non-destructive testing in this particular material, has been demonstrated in some studies [30,47]. Their main conclusion was that the pre-established ratios between compressive strength and the indirect measures, suitable for conventional concretes, were not applicable. Despite that conclusion, no precise general relationships have up until now been established between indirect measurements and the compressive strength of SCC.

As observed above, the validity of the indirect measures on SCC containing RCA has many shortcomings, especially when used in the fine fraction, which has a particular impact in the case of the SCC. The main objective of this research work is to establish whether the compressive strength of SCC containing high amounts of both coarse and fine RCA can be accurately estimated by both the hammer rebound index and UPV analysis. Moreover, among the various possible SCC flowabilities, an SF3 slump-flow class [49] (very high flowability) was chosen, due to its extreme proportion of fines and powder compared to vibrated concrete [50], which can to a greater extent alter the validity of indirect measures to predict compressive strength.

Furthermore, this research is part of a larger project for the evaluation of different aspects of recycled self-compacting concretes (100% coarse RCA), and it is linked to other novel aspects such as the effect of the addition of alternative binders, in this case Ground Granulated Blast Furnace Slag (GGBFS), and different types of aggregate powder. In the present paper, this aspect is leveraged, to test the consistency of the indirect measures regardless of any change in the composition of the SCC mixtures.

The final purpose of this paper is to develop models that can be used to estimate the compressive strength of SCC containing RCA with similar levels of reliability to conventional concrete, so that the strength monitoring by non-destructive testing of this material is possible in any structure. In doing so, the authors aim to promote the actual use of SCC containing RCA.

The compressive strength, the hammer rebound index, and the UPV of 24 SCC mixtures were determined at 1, 7, 28, and 90 days for the evaluation and the analysis of all the aspects addressed above, in order to analyze all the aspects addressed. These mixes were manufactured with 100% coarse RCA, and 0, 50, or 100% fine RCA, as well as two different types of cement (CEM I and CEM III/A, this last one with around 45% of GGBFS) and four different types of aggregate powder (limestone filler, two sizes of limestone fines, and RCA).

1.1. Novelty of the study

In view of the above discussion throughout the introduction, this study presents the following novelties:

- Firstly, it demonstrates the validity of indirect measures (hammer rebound index and UPV) to estimate the compressive strength of SF3 class SCC. This type of concrete, with a highly particular mix design, has never before been subjected to this type of analysis.
- Secondly, it evaluates the effect of several combinations of fine RCA content, type of binder, and aggregate powder in the relationship between compressive strength and indirect measures in highly SCC. These components are of immense importance in the behavior of SCC, due to its high content of fine particles, and therefore condition the validity of the indirect measurements. Studies on SF2 class SCC have to date only focused on coarse RCA content.
- Finally, this study is the first one that provides suitable models to estimate the compressive strength of SCC through non-destructive testing regardless of its composition.

2. Materials and methods

The raw materials and the experimental procedure used to obtain the results are detailed in this section, before moving on to the presentation of the experimental results.

2.1. Materials

The main characteristics of the raw materials (cement, aggregates, admixtures, and water) used for the manufacture of SCC are set out below.

2.1.1. Cement, water, and admixtures

Both CEM I 52.5 R (density 3.12 Mg/m³) and CEM III/A 42.5 N (density 3 Mg/m³), from among the various cement types specified in standard EN 197-1 [51], were used. The main difference between them was the presence of Ground Granulated Blast Furnace Slag (GGBFS) in the CEM III/A (content around 45%). Water was used from the mains water supply of Burgos, northwestern Spain, where the experiment was performed. Two admixtures were used to optimize the SCC: a viscosity regulator, referred to here as "Adx1", that retains long-term flowability, and a plasticizer water reducer, "Adx2".

2.1.2. Natural and recycled aggregates

The SCCs developed in this study contained high volumes of RCA: 100% of the coarse fraction (4/12 mm) and 0, 50, or 100% of the fine fraction (0/4 mm). The RCA consisted of crushed precast concrete elements at a local waste treatment company, rejected due to aesthetic defects. Its average strength was 45 MPa. They were received in the laboratory with a continuous grain size of 0/31.5 mm, which was separated by sieving into three different fractions (0/4, 4/12.5, and 12.5/31.5 mm), the first two of which were used in this study. The fine aggregate content was completed by the addition of siliceous sand 0/4 mm, usually used for SCC production in the region.

Limestone filler is generally used as aggregate powder in the manufacture of SCC [45]. Nevertheless, in this study, four aggregate powders were compared in terms of their performance: limestone filler < 0.063 mm, commercial limestone fines 0/1 mm, limestone fines 0/0.5 mm, and RCA 0/0.5 mm. The last two materials were graded by sieving limestone fines 0/1 mm and RCA 0/4 mm, respectively.

The density and water absorption of these aggregates, as per EN 1097-6 [51], are shown in Table 1. Two aspects of the test should be considered, regarding the determination of aggregate water absorption. Firstly, water absorption in 15 and 45 min was determined without prior drying of the aggregates in an oven, so the results could be assimilated to the water absorption of the aggregate during mixing. Secondly, the fine RCA was continuously moved during the drying process to avoid the onset of setting during this test. From a comparison of the results, it can be observed that, as expected, RCA had a lower density and higher water absorption than NA [41]. Finally, the granulometry curves of all these aggregates are shown in Fig. 3.

2.2. Mix design

A total of 24 different mixtures were prepared from combinations of the different types of cement, the aggregate powder, and the fine RCA percentages. All the aggregates were used under environmental conditions (they were stored in the laboratory throughout the study), to assimilate the mixing of the SCC to the most common method used in concrete plants [52]. An SF3 slump-

Table 1
Density and water absorption of the aggregates.

Aggregate	Saturated-Surface-Dry (SSD) Density (Mg/m^3)	15 min water absorption (%)	45 min water absorption (%)	24 h water absorption (%)
Coarse RCA 4/12.5 mm	2.42	4.90	5.35	6.25
Fine RCA 0/4 mm	2.37	5.77	6.34	7.36
Siliceous sand 0/4 mm	2.58	0.18	0.22	0.25
Limestone fines 0/1 mm	2.62	1.88	2.12	2.53
Limestone fines 0/0.5 mm	2.60	1.95	2.26	2.57
RCA 0/0.5 mm	2.31	6.32	6.94	7.95
Limestone filler < 0.063 mm	2.77	–	–	0.54
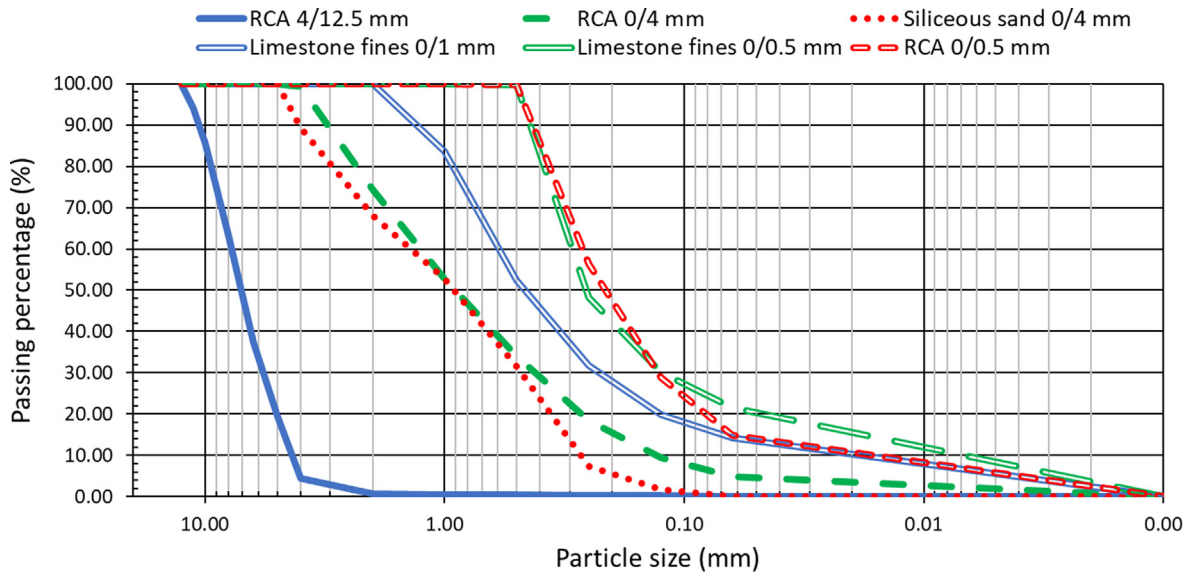
Fig. 3. Aggregate size distribution.

flow class (maximum diameter between 750 and 850 mm) [49] in all mixtures was obtained with the following design criteria:

- First, the overall particle size, especially of the finest fractions (size less than 0.250 mm), was adjusted to the Fuller curve to reach self-compactability. This is shown in Fig. 4 for mixtures made with CEM I and 50% fine RCA.
- The initial water content was defined according to EFNARC recommendations [49] and empirically adjusted in trial mixtures with 100% coarse RCA and 0% fine RCA before producing the final mixtures. An effective water-to cement ratio of 0.50 in mixes with CEM I and 0.40 in mixes with CEM III was established. These amounts of water were adjusted in each mix with fine RCA (0/4 mm and/or 0/0.5 mm) to maintain the effective water-to-cement ratio constant. To that end, the additional water incorporated in each mixture corresponded to the results of the water absorption test of the RCA in 15 min (see Table 1), which was the mixing time (see Section 2.3).
- Furthermore, the coarse RCA was reduced in the mixtures with CEM III/A, to enhance flowability, as the highly ground fineness of CEM III/A hindered the drag force of the larger aggregate particles.

All these aspects led to the development of the mix design that is shown in Table 2. The mixtures were labelled C-N/T, which means:

- C refers to the type of cement used: I (CEM I) or III (CEM III/A).
- N refers to the percentage of RCA 0/4 mm incorporated in the mixture: 0, 50, or 100%.

- T refers to the type of aggregate powder: F (limestone filler), M (mix of limestone filler and limestone fines 0/1 mm), L (limestone fines 0/0.5 mm), and R (RCA 0/0.5 mm). The use of only limestone fines 0/1 mm as aggregate powder was insufficient to reach an SF3 slump-flow class and had to be combined with limestone filler.

2.3. Experimental procedure

Staged mixing processes are useful for maximizing both component hydration and, therefore, SCC flowability levels [53]. They are especially useful when aggregates with high water absorption are incorporated, such as fine RCA [54]. Hence, in this research, the components of the mixtures were added in three different stages during the mixing process. Each stage was followed by 3 min of mixing and 2 min of inactivity. These durations were determined after testing different mixing and inactivity times between 1 and 5 min, to maximize flowability [52]. The total duration of this mixing process was 15 min and the stages were as follows:

- Stage 1: addition of the aggregates (coarse RCA, siliceous sand and/or fine RCA, and aggregate powder) and half of the water.
- Stage 2: addition of cement and remaining water
- Stage 3: addition of admixtures.

Having completed this process, the self-compactability over time of the mixes (initial class SF3) was checked with the slump-flow test at 0 and at 30 min, and 12 cubic 10 × 10 × 10-cm specimens were produced for each mixture.
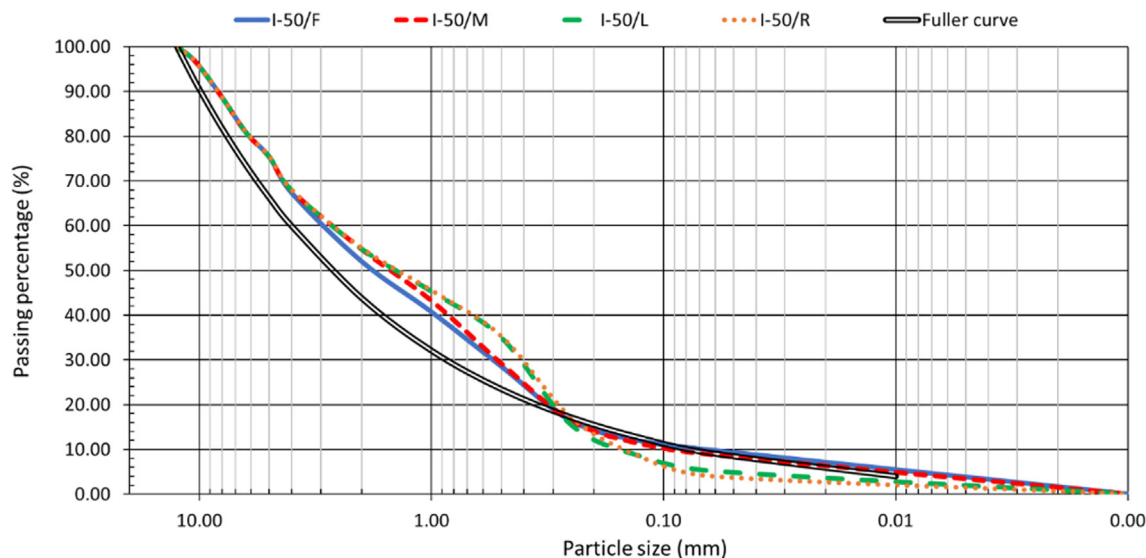
Fig. 4. Joint granulometry of the mixes with 50% fine RCA and CEM I.

Table 2
Mix design (weights in kg).

	Mixtures with CEM I			Mixtures with CEM III/A		
CEM I	300			0		
CEM III/A	0			425		
RCA 4/12.5 mm	530			430		
Adx1	2.30					
Adx2	4.50					
	I-0/F	**I-50/F**	**I-100/F**	**III-0/F**	**III-50/F**	**III-100/F**
Limestone filler < 0.063 mm	165					
Water	185	210	235	185	210	235
RCA 0/4 mm	0	505	1010	0	505	1010
NA 0/4 mm	1100	550	0	1100	550	0
	I-0/M	**I-50/M**	**I-100/M**	**III-0/M**	**III-50/M**	**III-100/M**
Limestone filler < 0.063 mm	115					
Limestone fines 0/1 mm	225					
Water	185	210	235	185	210	235
RCA 0/4 mm	0	435	865	0	435	865
NA 0/4 mm	940	475	0	940	475	0
	I-0/L	**I-50/L**	**I-100/L**	**III-0/L**	**III-50/L**	**III-100/L**
Limestone fines 0/0.5 mm	335					
Water	185	210	235	185	210	235
RCA 0/4 mm	0	435	865	0	435	865
NA 0/4 mm	940	475	0	940	475	0
	I-0/R	**I-50/R**	**I-100/R**	**III-0/R**	**III-50/R**	**III-100/R**
RCA 0/0.5 mm	305					
Water	200	220	245	200	220	245
RCA 0/4 mm	0	435	865	0	435	865
NA 0/4 mm	940	475	0	940	475	0

The specimens were stored in a moist room (95 ± 5% humidity and 20 ± 2 °C temperature) to achieve optimum strength development. Three days before each age testing, the specimens were exposed to the laboratory environment (60 ± 5% humidity and 20 ± 2 °C temperature), to obtain a completely dry concrete surface [2]. The real conditions of the structure when its compressive strength is indirectly estimated were thereby simulated [3].

The hammer rebound index, the UPV analysis, and the compressive strength of 3 test specimens were determined at 1, 7, 28, and 90 days. The results at each age and mix were obtained as the arithmetic mean of these values. The testing of all SCCs at four dif-

ferent ages meant that this study covered a wide range of strengths. The hardened density was also determined at 28 days.

The experimental plan and its link to the results, discussed in Section 3, are shown in the flowchart of Fig. 5.

2.4. Relationship between indirect measurements and compressive strength in conventional concretes

In this study, a Schmidt hammer type N was used for the measurement of the hammer rebound index. The compressive strength of the non-recycled vibrated concrete can be estimated from
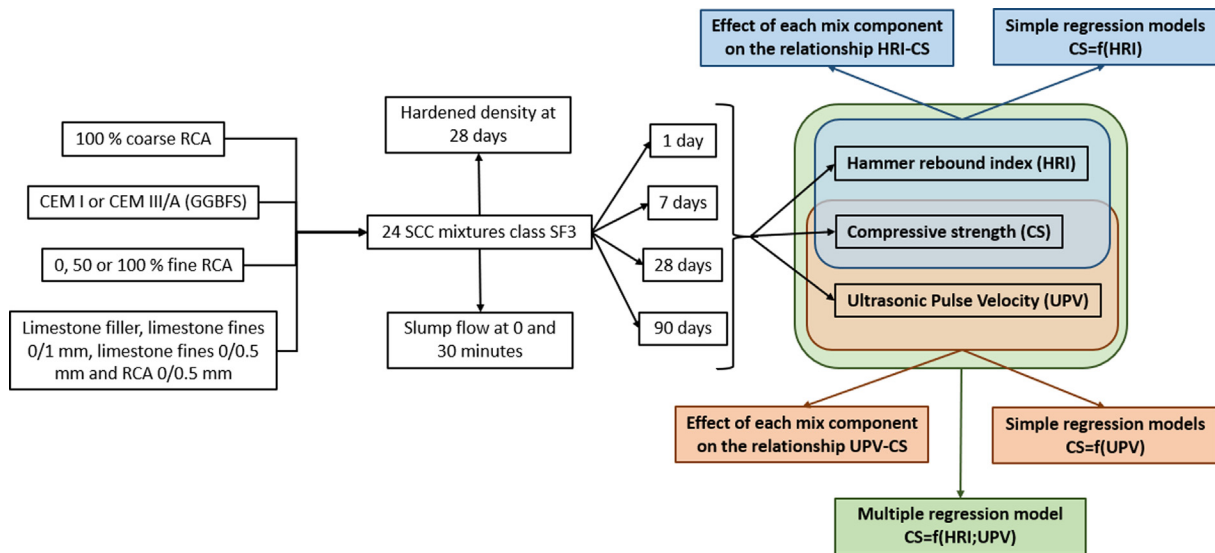
Fig. 5. Flowchart of the study: experimental plan versus experimental results.

Table 3 [55] as a function of the rebound index obtained with this type of Schmidt hammer. The values within this table were obtained by statistical fitting of large data volumes, a fundamental aspect for the validity of these models [56], as stated in the introduction.

There is no one standard calibrated UPV model. However, the relationships shown below are generally established between the UPV and the compressive strength values [13], although the hammer rebound index is generally recommended to complement the UPV values [5].

- Low-strength concrete: 2.5–3.2 km/s.
- Medium-strength concrete: 3.2–3.7 km/s.
- High-strength concrete: 3.7–4.2 km/s.
- Very high-strength concrete: >4.2 km/s.

3. Results and discussion

In this section the fresh performance of the SCCs designed are presented. Then, the results of compressive strength, the hammer rebound index, and UPV, as well as the relationships between these variables are analyzed.

3.1. In-fresh performance: slump-flow test

The slump flow, EN 12350-8 [51], of each mix, obtained at 0 and at 30 min after the mixing process had ended, is shown in Fig. 6 to an accuracy of ± 5 mm. As has been indicated in the mix design section, an SF3 slump-flow class [49] at 0 min was imposed as a design criterion. On the other hand, 30 min later, most of the mixes were of class SF2 (maximum diameter between 650 and 750 mm), except for mixes I-50/R and I-100/R, which did not reach the value of 650 mm (slump-flow class SF1). The behavior of these two mixes was mainly due to the high water absorption of the RCA, which was used in these mixes as fine aggregate and aggregate powder

The three variables introduced in the composition of the mixtures (type of cement, fine RCA content, and nature of the aggregate powder) influenced the slump-flow evolution in a different way:

- In mixtures with CEM III/A, the lower coarse aggregate proportion (see Section 2.2) eased the dragging of all the components of the mixture by the cement paste [57], which in turn led to a higher slump flow at both moments in time.

Table 3
Estimation of compressive strength as a function of the hammer rebound index on cubic specimens in vibrated concrete manufactured with NA.

Hammer rebound index	Concrete age: 7 days		Concrete age: > 7 days		Hammer rebound index	Concrete age: 7 days		Concrete age: > 7 days		Hammer rebound index	Concrete age: 7 days		Concrete age: > 7 days	
	W_m	W_{min}	W_m	W_{min}		W_m	W_{min}	W_m	W_{min}		W_m	W_{min}	W_m	W_{min}
20	9.9	5.3	11.9	7.3	31	25.2	18.9	26.4	20.1	41	42.4	35.2	42.6	35.4
21	11.1	6.3	12.9	8.1	32	26.9	20.5	28.0	21.6	42	44.1	37.0	44.2	37.1
22	12.4	7.4	14.2	9.2	33	28.5	22.1	29.4	23.0	43	46.0	38.7	46.1	38.8
23	13.6	8.4	15.4	10.2	34	30.1	23.5	30.9	24.3	44	47.9	40.6	47.9	40.6
24	14.9	9.6	16.6	11.3	35	31.8	25.1	32.5	25.8	45	49.7	42.4	49.7	42.4
25	16.3	10.8	18.0	12.5	36	33.5	26.8	34.1	27.4	46	51.6	44.2	51.6	44.2
26	17.7	12.0	19.2	13.5	37	35.3	28.4	35.8	28.9	47	53.5	46.1	53.5	46.1
27	19.1	13.2	20.6	14.7	38	37.0	30.1	37.4	30.5	48	55.4	48.0	55.4	48.0
28	20.6	14.6	22.1	16.1	39	38.7	31.8	39.0	32.1	49	57.3	49.8	57.3	49.8
29	22.1	16.0	23.4	17.4	40	40.5	33.4	40.8	33.7	50	59.2	51.7	59.2	51.7
30	23.6	17.5	24.9	18.7										

W_m: most likely compressive strength value (MPa)
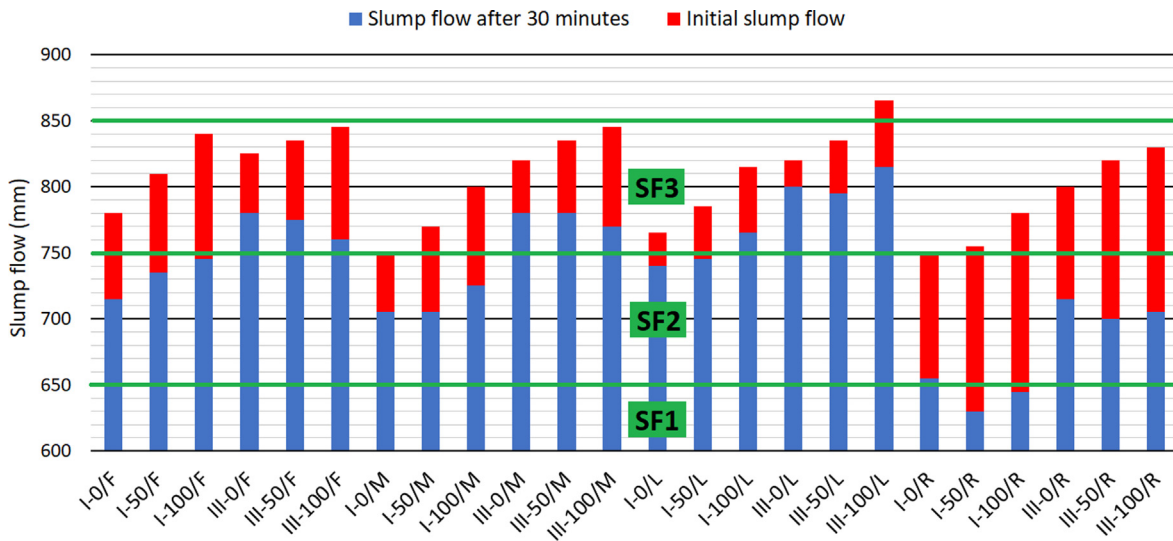W_{min}: minimum expected compressive strength value (MPa)

Fig. 6. Slump flow 0 and 30 min after the end of the mixing process.

- The high fines proportion of the fine RCA, compared to siliceous sand, increased the initial slump flow. Nevertheless, the high water absorption worsened its temporary conservation, as other researchers had previously observed [54].
- In relation to the different types of aggregate powder, the use of limestone filler caused a higher initial slump flow (F-mixes). However, a lower temporal slump-flow loss was obtained with the use of limestone fines 0/0.5 mm (L-mixes). The high water absorption levels of the RCA filler (see Table 1) resulted in the worst behavior, obtained for the R-mixes, as has also been observed by other authors [58], regardless of the type of cement or the percentage of fine RCA. The pre-soaking of the RCA could have improved this behavior by reducing the water absorption of this waste after the mixing process [52].

The parameter t_{500} (time to reach a slump flow greater than 500 mm), also obtained in the slump-flow test, was used to evaluate the viscosity of the SCCs. In this study, these values were obtained to an accuracy of ± 0.2 s. As may be observed in Fig. 7, all the concrete mixtures presented an initial viscosity of class VS2 (time to reach a slump flow of 500 mm higher than 2 s), although mixtures III-0/F and III-0/L were of class VS1 (values of 1.6 and 1.8 s, respectively). After 30 min, all mixtures were class VS2, clearly showing the effects of all the changes within the composition:

- CEM III/A, which incorporated GGBFS, reduced the initial viscosity. However, the mixes with CEM III/A had a greater temporal increase in viscosity than mixes with CEM I. This fact is due to the properties of GGBFS that usually hinder the temporary preservation of viscosity [59].
- The addition of fine RCA increased the viscosity both initially and at 30-minutes. Mixtures with 100% fine RCA were the most viscous. These observations are in line with the conclusions reached in studies on the effect of fine RCA on the temporal evolution of the rheology of the SCC [60].
- The aggregate powder influenced the viscosity of the mixtures in the same way as in the slump flow. Initially, the mixtures with limestone filler were the least viscous. However, due to the electrostatic charge that the limestone filler acquires during its manufacture [61], the smallest temporary increase in viscosity was in the L-mixes. According to this, the M-mixes showed an intermediate behavior. Finally, the irregular shape of the

RCA filler [62] and its high water absorption [58] resulted in the highest initial viscosity and the largest temporary increase in the R-mixes.

These slump-flow and viscosity results show that a careful design of the mixture means that the concretes can achieve a high initial workability, even if RCA (in the coarse, fine, and powder fractions) and GGBFS are simultaneously used [63]. However, the addition of these by-products complicate the temporary conservation of SCC flowability levels [54,64]. Moreover, their adverse effects appeared to increase when they were jointly used. From the results, it can be concluded that concrete mixtures with 50% fine RCA optimized their slump flow, and viscosity simultaneously, as well as their temporary conservation, regardless of the binder or the natural aggregate powder in use. These optimum amounts of RCA are in accordance with the results of other authors [33], whose recommendations were never to exceed an RCA content of 50% in the fine fraction when the whole coarse fraction is RCA [65].

3.2. Hardened density

The hardened density of each mix, determined according to EN 12390-7 [51], is shown in Table 4. These values showed the expected trends. Firstly, the hardened density of concrete was reduced when RCA, regardless of its fraction, was used, due to its lower density compared to NA, a widely reported aspect in the literature [54]. Secondly, the increase of the amount of mix water when RCA was added also favored the decrease of the hardened density [41]. Finally, the hardened density increased in mixtures with CEM III/A, due to their higher content of cement, which is denser than coarse RCA.

3.3. Compressive strength

SCC flowability and strength are very sensitive to changes in the mix composition, even more so if by-products are incorporated [45]. Therefore, it is essential to obtain a balance between flowability and strength through a correct mix design [66]. In this study, the main objective was to achieve SCCs with a SF3 slump-flow class, so the amount of water was adapted when the fine RCA content increased, to compensate its high water absorption and to maintain high flowability of the SCC, but at the same time to achieve a suitable compressive strength [41]. As a result of both
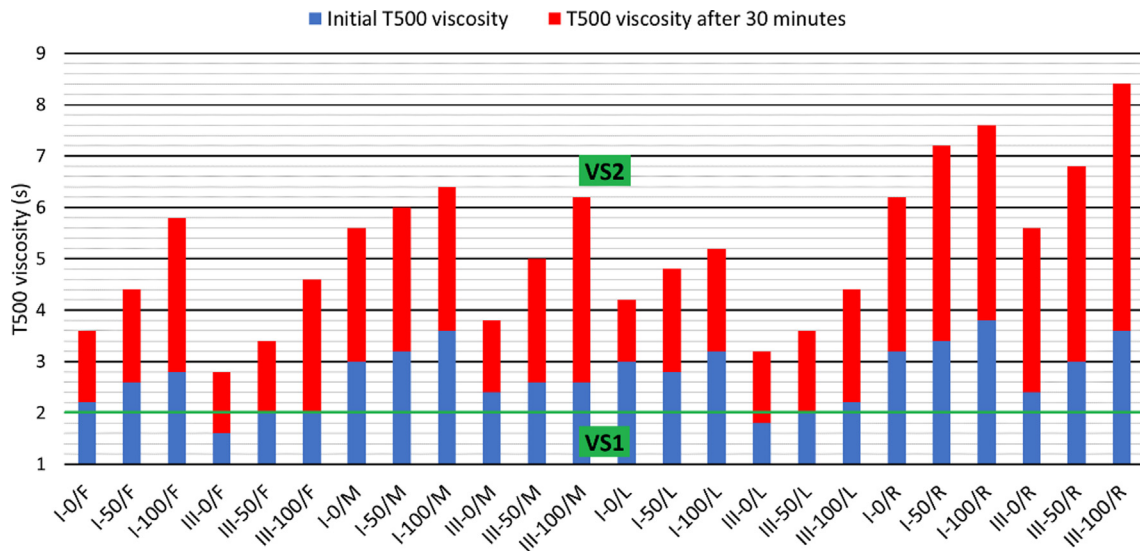
Fig. 7. T_{500} viscosity at 0 and at 30 min after the end of the mixing process.

Table 4
Hardened density of the mixes (Mg/m³).

	/F	/M	/L	/R
I-0	2.26	2.24	2.24	2.15
I-50	2.19	2.17	2.09	1.95
I-100	2.05	1.97	1.93	1.76
III-0	2.30	2.27	2.24	2.15
III-50	2.23	2.21	2.16	2.08
III-100	2.12	2.07	2.02	1.81

the fine RCA addition and the increase of the water content [41], the compressive strength decreased at all ages (1, 7, 28, and 90 days) when this waste was used, as shown in Fig. 8. The addition of 50% fine RCA caused a decrease in strength of around 2–7 MPa at 90 days, compared to mixtures without this by-product. This decrease was 10–20 MPa for mixes with 100% fine RCA. Therefore, the decrease in strength was not proportional to the amount

of fine RCA that was added [33], which could be due to the adjustment of the water content of the mixture, which differed for each fine RCA content [39].

The use of GGBFS, rather than causing a decrease, led to an increase in strength, despite the lower clinker content of the mixes (assuming a clinker content of 95% for CEM I and 55% for CEM III/A, according to EN 197-1 [51], the clinker content in mixtures with CEM I was 285 kg/m³, and only 235 kg/m³ in mixtures with CEM III/A). These results demonstrated the good behavior of GGBFS as a binder [67], even when it was combined with coarse and fine RCA [63].

The mixtures with the same type of cement and fine RCA content, but with different natural aggregate powders (limestone filler, mix of limestone filler and limestone fines 0/1 mm, or limestone fines 0/0.5 mm), had very similar strengths at 90 days, and showed trends with regard to the fine RCA content that have also been observed in other studies [65]. However, the values obtained in the L-mixes were slightly higher. The use of RCA 0/0.5 mm pro-
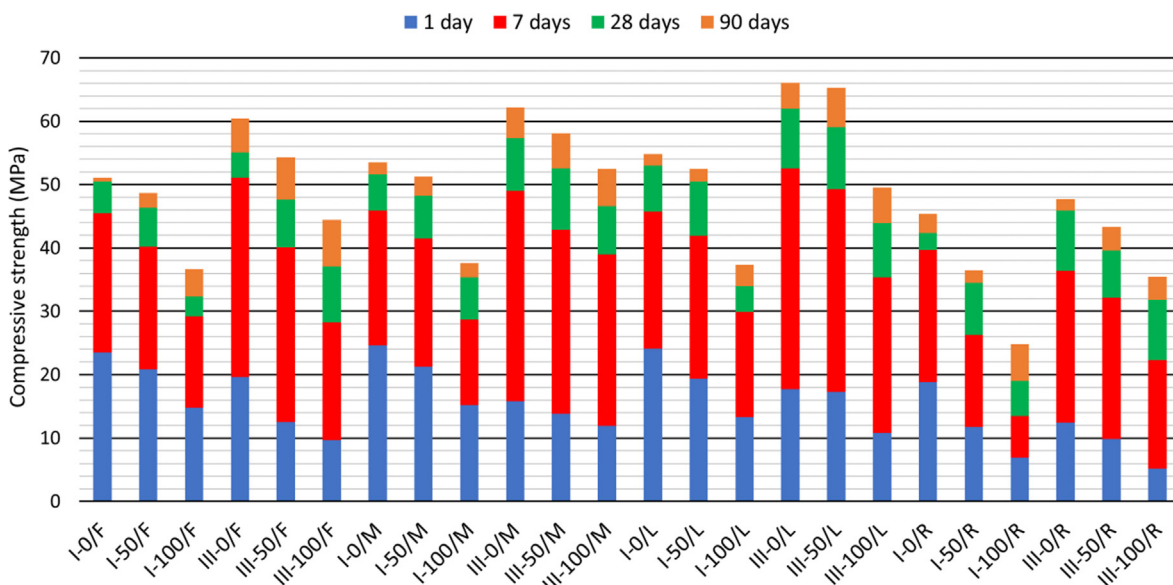

Fig. 8. Compressive strength at 1, 7, 28, and 90 days on cubic specimens.

vided the worst results, although mixtures I-0/R, III-0/R, and III-50/R had final strengths of over 45 MPa. Mixture I-100/R was the only one not to reach a compressive strength of 30 MPa at 90 days.

In addition to the compressive strength values that were obtained, it is possible to analyze the effect of each mix component on the temporal evolution of this strength (Fig. 9). The mixtures manufactured with CEM III/A presented a higher final strength (Fig. 8), although they showed a slower temporal evolution. This effect of the GGBFS is reported by both standards, such as EN 197-1 [51], and studies that evaluated the effect of the joint use of RCA and GGBFS [59]. Moreover, the addition of fine RCA also delayed the acquisition of strength [41]. Thus, the mixtures containing CEM I, natural aggregate powder, and 100% siliceous sand 0/4 mm developed 83–89% of their strength at 7 days. Nevertheless, the same mixtures, but with 100% fine RCA developed only 76–80% of their final strength. This effect was more notable when fine RCA and GGBFS were simultaneously used: mixes with CEM III/A and 100% fine RCA had developed only 63–74% of their final strength at 7 days. The use of RCA 0/0.5 mm further delayed the development of strength: at 7 days, mixture I-100/R presented only 54% of its strength at 90 days.

From all aspects addressed in this section, a clear conclusion can be obtained: the addition of 50% fine RCA (in mixtures with 100% coarse RCA) resulted in minimal decreases in strength. In addition, the flowability of these mixtures was adequate (see Section 3.1). Therefore, the authors of this article considered that the most suitable fine RCA content in this study was 50%. The addition of GGBFS to these mixtures was also adequate, because this alternative binder yielded high compressive strengths.

3.4. Hammer rebound index

Similar to the compressive strength, the hammer rebound index was determined at 1, 7, 28, and 90 days for all mixes. The hammer rebound index of each specimen was obtained as the median of nine determinations, according to EN 12504-2 [51]. The overall result of each mixture at each age was the arithmetic mean of three test specimens (Table 5). Therefore, a total of 2592 hammer rebound tests were performed, considering all the specimens, ages, and mixtures.

The increase in compressive strength resulted, as expected, in an increase in the hammer rebound index [47]. The increase in the hammer rebound index of the SCC produced with GGBFS was higher than expected in view of the trends shown by the models developed for non-recycled concrete (see Table 3). In the mixes produced with GGBFS, the surface hardness depended mainly on the binder instead of the coarse aggregate. Therefore, the hydration process of the binder led to higher increases of the hammer rebound index.

Furthermore, the value of the hammer rebound index at each age depended on the type of binder in use. Mixes with CEM I developed almost all its compressive strength at 28 days, so the results at 28 and 90 days were very similar. Nevertheless, mixes with CEM III/A underwent a higher evolution of the hammer rebound index, because of its slower strength development. Finally, the addition of RCA, with a lower surface hardness than NA, also caused the hammer rebound index to decrease [44] regardless of whether it was added as fine aggregate or aggregate powder.

3.4.1. Model of the relationship between the hammer rebound index and compressive strength in conventional concretes

As explained in Section 2.4, the model shown in Table 3 was obtained for vibrated concrete made with NA [55]. The compressive strengths of the cubic concrete specimens of this study were estimated with that model as a function of the hammer rebound index, and the results are shown in Fig. 10. This figure is a comparative graph between the observed value of compressive strength results, shown in Fig. 9, and the estimated strength at different ages through the hammer rebound index, using the model given in Table 3. The bisector indicates the points at which the observed strength was equal to the estimated strength. If the points are above this bisector, the observed values were greater than the estimated ones.

The first general observation on the basis of this figure is that, using this conventional model (Table 3), the compressive strength was, in all cases, underestimated. The high content of fine aggregate and aggregate powder required to produce a SF3 class SCC [45] showed that it had a lower surface hardness than expected and, therefore, the hammer rebound indexes were also lower. This effect was generally greater in mixtures made with CEM III/A, due to their lower amount of coarse aggregate. Moreover, the existing model underestimated the compressive strength by approximately 15 MPa (30–40%), for observed compressive strengths of 20–50 MPa. When the observed strength was higher than
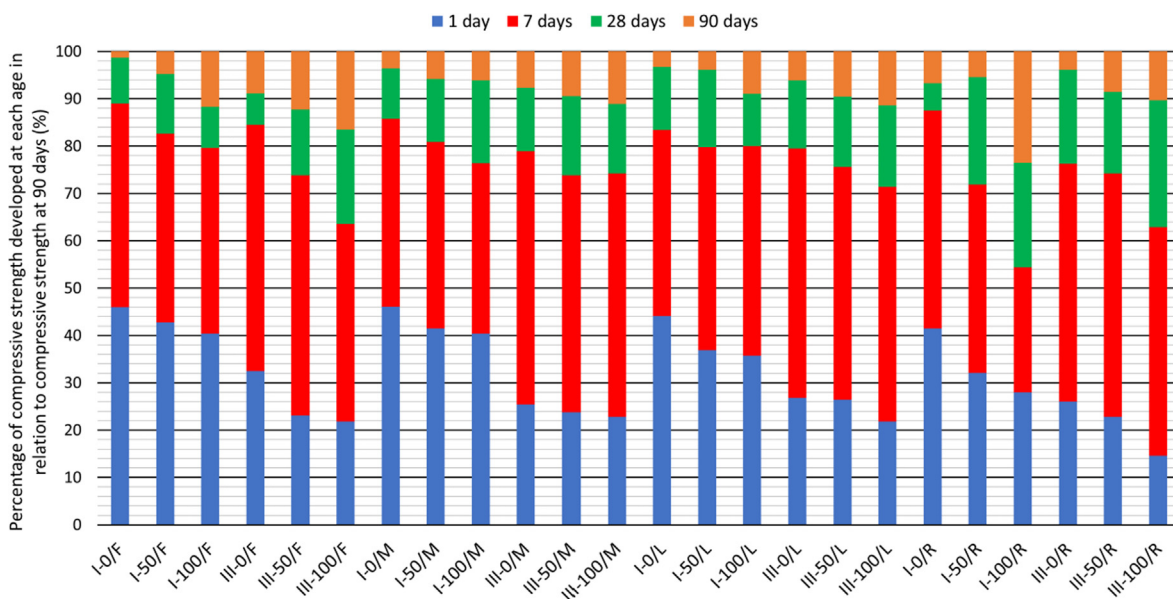

Fig. 9. Percentage compressive strengths at 1, 7, 28, and 90 days.

Table 5
Hammer rebound index values at 1; 7; 28; 90 days.

	/F	/M	/L	/R
I-0	25; 34; 39; 40	25; 35; 39; 42	24; 33; 41; 42	17; 28; 29; 32
I-50	23; 30; 34; 37	23; 31; 34; 41	20; 31; 40; 41	12; 22; 26; 28
I-100	19; 26; 28; 32	20; 26; 29; 31	18; 26; 29; 30	10; 12; 18; 21
III-0	20; 39; 42; 45	17; 36; 42; 46	18; 40; 46; 48	11; 28; 31; 32
III-50	17; 31; 33; 41	15; 31; 40; 43	17; 38; 45; 48	10; 26; 28; 30
III-100	14; 25; 30; 32	15; 31; 33; 40	13; 27; 32; 34	10; 20; 26; 27
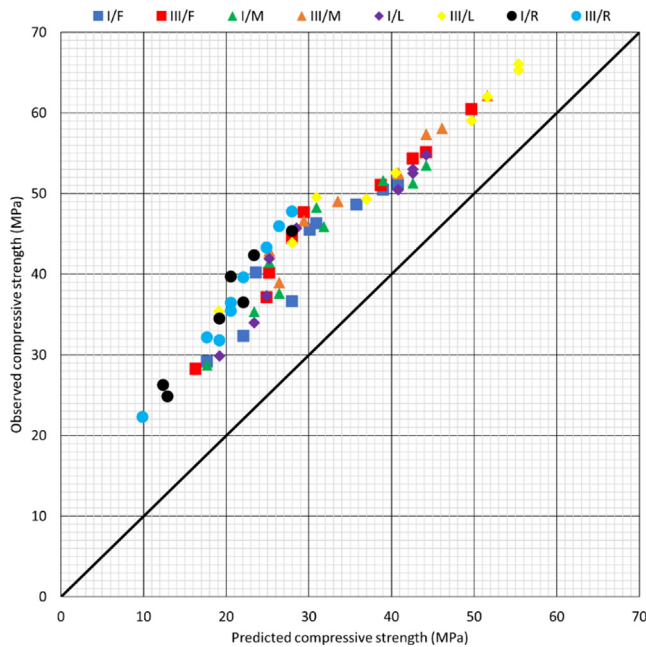
Fig. 10. Relationship between the predicted compressive strength with the hammer rebound index, according to Table 3, and the experimental results of compressive strength.

50 MPa, the strength underestimations of the model were around 10 MPa (15–20%). Most of the mixes with compressive strengths of between 20 and 50 MPa incorporated fine RCA and/or RCA filler. Hence, it appeared that RCA increased this underestimation, due to its lower hardness compared to NA [44]. From these results, it can be concluded that the models developed for vibrated concrete were not valid for SF3 class SCC, so in the next section the development of new models for this type of concrete will be studied. The final aim will be to obtain a single model valid for recycled SCC of high-flowability regardless of its composition.

3.4.2. Development of a new model for the relationship between the hammer rebound index and compressive strength

In view of the results set out in the previous section, a particular model is needed to estimate compressive strength as a function of the hammer rebound index in SF3 class SCCs containing RCA. Firstly, the two best-fit models for the relationship between both variables (*CS*, Compressive Strength, in MPa; and *HRI*, Hammer Rebound Index) are presented in Table 6, distinguishing between the different variations introduced in the composition of the mixtures (type of cement, fine RCA content, and nature of the aggregate powder).

It can be seen that an optimal adjustment was obtained, with coefficients R^2 of over 95% in almost all cases. Therefore, the compressive strength of the SCC can be accurately estimated by the hammer rebound index regardless of its composition, as other studies have suggested in relation to the coarse and fine RCA content [47]. On the other hand, it is also possible to analyze the effect that each change in the composition of the mixture has on the relationship between these two variables:

- Modification of the type of cement or fine RCA content (up to percentages of 50%) led to no change in the nature of the models with the best fit, which means that models with the same expression were obtained, according to Eq. (1). The only difference between them was the value of the coefficients (a, b).

$$CS = \sqrt{a + b \cdot HRI^2} \qquad (1)$$

Table 6
Adjustment of compressive strength (MPa) as a function of the hammer rebound index.

		Model expression	Coefficient R^2 (%)
Mixes with the same type of cement	Mixes with CEM I	$CS = \sqrt{-270.40 + 1.86 \cdot HRI^2}$	94.38
		$CS = -10.00 + 1.56 \cdot HRI$	94.08
	Mixes with CEM III/A	$CS = \sqrt{-178.11 + 1.93 \cdot HRI^2}$	97.93
		$CS = -8.62 + 1.57 \cdot HRI$	97.64
Mixes with the same fine RCA content	Mixes with 0% RCA 0/4 mm	$CS = \sqrt{-197.39 + 1.90 \cdot HRI^2}$	96.06
		$CS = -7.66 + 1.53 \cdot HRI$	95.39
	Mixes with 50% RCA 0/4 mm	$CS = \sqrt{-185.55 + 1.86 \cdot HRI^2}$	96.21
		$CS = -8.03 + 1.53 \cdot HRI$	95.92
	Mixes with 100% RCA 0/4 mm	$CS = \left(-2.55 + 1.58 \cdot \sqrt{HRI}\right)^2$	95.49
		$CS = (1.00 + 0.17 \cdot HRI)^2$	95.37
Mixes with the same aggregate powder	Mixes with limestone filler	$CS = (-8.57 + 4.30 \cdot ln(HRI))^2$	97.30
		$CS = -63.45 + 18.41 \cdot \sqrt{HRI}$	96.95
	Mixes with limestone filler and limestone fines 0/1 mm	$CS = \left(-2.52 + 1.55 \cdot \sqrt{HRI}\right)^2$	96.83
		$CS = exp(-1.50 + 1.49 \cdot HRI)$	96.78
	Mixes with limestone fines 0/0.5 mm	$CS = \sqrt{-305.51 + 1.94 \cdot HRI^2}$	97.95
		$CS = -10.59 + 1.59 \cdot HRI$	97.79
	Mixes with RCA 0/0.5 mm	$CS = 5.37 + 0.04 \cdot HRI^2$	98.44
		$CS = -9.62 + 1.71 \cdot HRI$	97.64

- Nevertheless, the addition of 100% fine RCA or the use of a different aggregate powder resulted in a different formulation of the best-fit model in each case. It can therefore be stated that the surface hardness of the SF3 class SCC was mainly affected by changes to the finer aggregate fractions [43], as other studies have stated for SCC of lower flowability [47]. In consequence, the relationship between compressive strength and the hammer rebound index was changed.

Another relevant aspect shown in Table 6 is that, although the linear model (Eq. (2)) is not the best-fit model in any case, it is the model with the second better fit in 6 out of the 9 cases under study. A result that shows why previous attempts to relate the compressive strength and rebound rate in SCC to RCA, by considering exclusively linear equations, approximated this relationship quite accurately [47]. However, the accuracy of this estimate can be more precise by using equations with a slightly more complex formulation [21].

$$CS = a + b \cdot HRI \tag{2}$$

Notwithstanding the above, it is clear that a global model (without differentiating between the changes in the composition of the mixtures) that relates the indirect measure to compressive strength is needed. Each indirect measure could therefore be quickly and easily applied to real structures, thereby encouraging the use of recycled SF3 class SCC in building and civil works. In this study, the development of a global model was performed by fitting all the data (compressive strength and hammer rebound index of the 24 mixtures at the 4 testing ages) by simple regression. On the other hand, obtaining a single model may involve specific goodness-of-fit problems, i.e., even though its overall fit is correct, there may be some range of the independent variable for which the estimate is imprecise. For this reason, it is advisable to achieve greater accuracy by using at least two models.

According to the previous paragraph, Eqs. (3) and (4) show the two best-fit global models (coefficients R² around 96%) for the relationship between compressive strength and the hammer rebound indexes of the mixes of this study. In these models, the specific goodness-of-fit problems indicated above can be clearly observed. Despite the fact that model 1 had the best overall fit, its fit was worse than for model 2 in the hammer rebound indexes between 10 and 15 and higher than 45. Therefore, although whenever possible the best-fit model should be used, it is recommended to employ model 2 for hammer rebound indexes lower than 15. Both models are plotted in Fig. 11. These models have the same expressions (with different coefficients) as those obtained in most cases by individual analysis (Table 6): Eqs. (1) and (2). It shows that the adjustment of large volumes of data can filter out the influence of the mixture composition (mainly the different nature of the aggregate powder or the high fine RCA content) on this relationship. Therefore, the hammer rebound index can be successfully used to estimate the compressive strength of SF3 class SCC containing RCA, regardless of changes to its composition, with only one model.

$$CS = \sqrt{-247.45 + 1.92 \cdot HRI^2}, \quad if \quad 15 < HRI < 45 \tag{3}$$

$$CS = -9.53 + 1.57 \cdot HRI, \quad if \quad 10 < HRI < 15 \quad and \quad 45$$
$$< HRI < 50 \tag{4}$$

As previously indicated, each global model that is represented (see Fig. 11) better fits a different compressive strength range, so the optimal choice is a statistical combination of both (Eqs. (3) and (4), Fig. 11) in a single model, so that the estimation will be
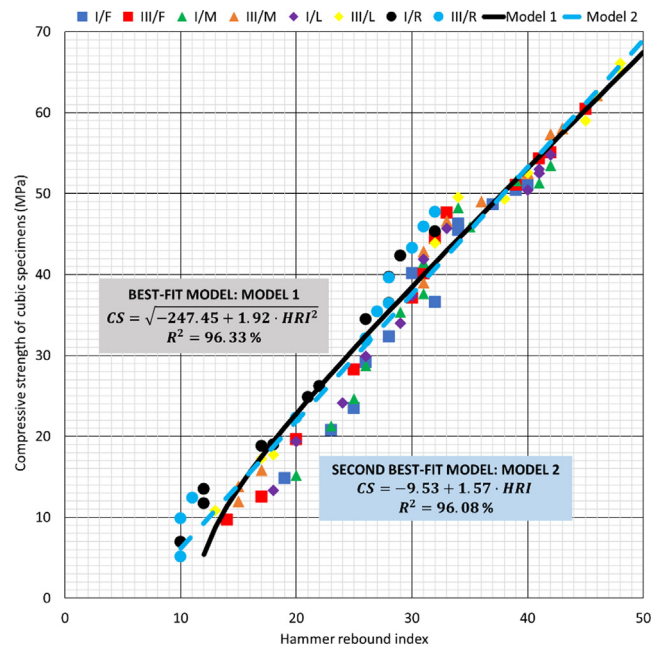

Fig. 11. Global models with the best fit for the relationship between compressive strength and the hammer rebound index.

as accurate as possible. In relation to this model, it is possible to go even further. If it is provided in table form it can be used immediately, with no need for mathematical operations (equations), which favors its quick use. For this reason and with the objective of assimilating the way of working on this type of concrete to that of conventional concrete (see Table 3), Table 7 shows the global combined model in table form. It collects both the most probable compressive strength on cubic specimens (W_m), and the minimum expected compressive strength at a 95% confidence level (W_{min}) as a function of the hammer rebound index.

In general, as can be observed in Fig. 12, the estimation of compressive strength using Table 7 is accurate. The worst fitting zone corresponded to an estimated compressive strength of 35–45 MPa, in which the observed compressive strength was underestimated by around 6 MPa. When the observed strength was overestimated, this strength was always higher than the minimum expected strength shown in Table 7. It demonstrates the validity of this model, with which the estimation is not only accurate, but also safe. Therefore, this model can be considered a first general approach to the use of the hammer rebound index for the estimation of compressive strength in real structures manufactured with recycled highly SCC.

3.5. UPV

The propagation speed (v) of an elastic wave in a continuous medium can be predicted by Eq. (5) (E, modulus of elasticity; ρ, density). In this relationship, the dependence on the Poisson coefficient (v) is a function of the boundary conditions [5]. However, it is also known that in a porous media such as concrete, the validity of this formulation can be uncertain, especially due to the capillary-type of porosity with singular pore-size distribution within both the matrix and the aggregates [41].

$$v = \sqrt{E/\rho} \cdot f(v) \tag{5}$$

Additionally, attempts to correlate the modulus of elasticity with the compressive strength is a classic problem in the field of

Table 7

Global model for the estimation of the compressive strength on cubic specimens as a function of the hammer rebound index.

Hammer rebound index	W_m	W_{min}	Hammer rebound index	W_m	W_{min}	Hammer rebound index	W_m	W_{min}	Hammer rebound index	W_m	W_{min}
10	6.2	0.0	21	24.0	15.0	31	39.6	33.6	41	54.7	49.5
11	7.7	1.0	22	25.6	17.3	32	41.1	35.2	42	56.2	51.1
12	9.3	1.9	23	27.1	19.3	33	42.6	36.8	43	57.7	52.6
13	10.9	2.9	24	28.7	21.3	34	44.1	38.5	44	59.2	54.2
14	12.5	3.9	25	30.3	23.2	35	45.6	40.1	45	60.7	55.7
15	14.0	4.8	26	31.9	25.0	36	47.2	41.7	46	62.2	57.3
16	15.6	5.8	27	33.4	26.8	37	48.7	43.3	47	63.7	58.8
17	17.3	6.8	28	34.9	28.5	38	50.2	44.8	48	65.2	60.3
18	19.0	7.7	29	36.5	30.2	39	51.7	46.4	49	66.7	61.9
19	20.7	8.7	30	38.0	31.9	40	53.2	48.0	50	68.2	63.4
20	22.3	12.5									

W_m: most likely compressive strength value (MPa)
W_{min}: minimum expected compressive strength value (MPa)
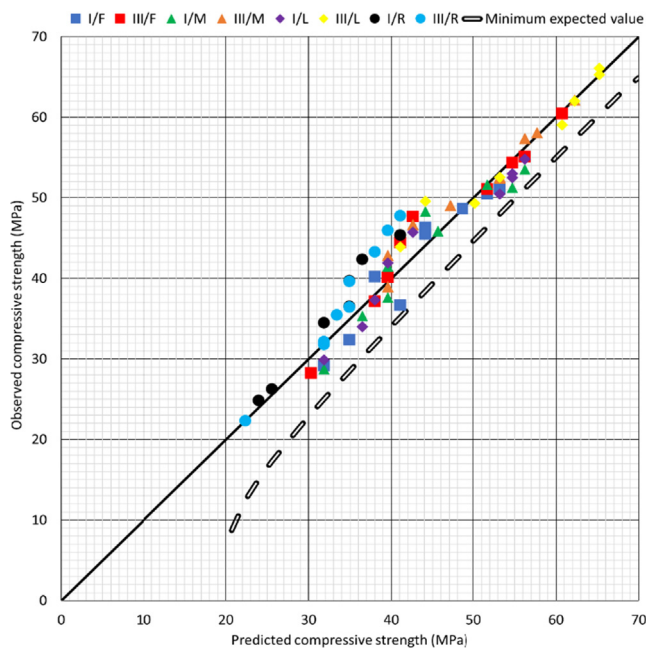
Fig. 12. Comparison between the predicted compressive strength with the hammer rebound index global model (Table 7) and the observed compressive strength.

concrete [56]. In view of the constraints of the literature [43,47], the authors of this study decided to study the direct correlation between the UPV values and the compressive strength of highly SCC.

UPV determination was performed according to EN 12504-4 [51]. The direct method was used (see Fig. 2). The UPV value for each specimen was obtained as the arithmetic mean of the UPV in the three spatial directions (X, Y and Z-axis). In addition, the overall result for each mix and age was the arithmetic mean of the UPV values of three specimens. In total, considering all the

specimens, ages, and mixes, 864 UPV measures were taken. The overall results obtained are shown in Table 8, according to which the UPV test results were higher than expected, which led to an overestimation of the compressive strength (see intervals of Section 2.4): UPV values greater than 4.2 km/s were obtained when none of the mixtures that were developed could be considered very high-strength concrete.

The UPV values clearly reflected the high compressive strength provided by CEM III/A at all ages. In fact, the results for mixtures with GGBFS were 5–10% higher than those of mixtures with CEM I. Nevertheless, this indirect measure did not accurately reflect the evolution of compressive strength at advanced ages in some cases, mainly when RCA 0/4 or 0/0.5 mm was incorporated. For instance, mixture III-50/R developed around 10% of its compressive strength between 28 and 90 days (see Fig. 9) and the UPV increased only 0.07 km/s.

3.5.1. Relationship between UPV and density

Very early [18] and more recent studies [30] have shown that an increase in the hardened density of concrete facilitates the propagation of ultrasonic pulses. In this study, the necessary reduction of the coarse aggregate content to obtain an SF3 slump-flow class resulted in a lower number of discontinuities within the concrete matrix, which affected this relationship [8].

In Fig. 13, the best-fit simple regression models (Eqs. (6) and (7)) between hardened density (*DEN*, in Mg/m^3) and UPV (km/s) are represented. Firstly, it can be seen that these models have a highly complex formulation and show a proportionally inverse relationship between both variables. Furthermore, a coefficient R^2 of only 69% was obtained, which makes the relationship between hardened density and UPV unclear. This performance is mainly due to the existence of a large number of mixes of different densities (2–2.3 Mg/m^3), but with a very similar UPV (3.8–4.2 km/s). It therefore appears that the high fines content of the SF3 class SCC created a very uniform medium for the propagation of ultrasonic waves [8], favoring similar UPV readings, despite the variation in density.

Table 8

UPV (km/s) at 1; 7; 28; 90 days.

|	/F	/M	/L	/R
I-0	3.28; 4.03; 4.12; 4.15	3.41; 4.05; 4.17; 4.11	3.45; 4.02; 4.22; 4.33	3.00; 3.90; 3.95; 4.02
I-50	3.17; 3.96; 4.05; 4.08	3.20; 3.95; 4.10; 4.17	3.07; 4.00; 4.09; 4.18	2.72; 3.35; 3.87; 3.94
I-100	2.81; 3.53; 3.71; 3.87	2.92; 3.46; 3.82; 3.90	2.77; 3.59; 3.82; 3.89	2.55; 2.77; 2.98; 3.33
III-0	3.09; 4.17; 4.30; 4.57	2.94; 4.10; 4.48; 4.61	2.77; 4.21; 4.63; 4.77	2.82; 3.83; 4.03; 4.07
III-50	2.74; 3.98; 4.07; 4.28	2.90; 3.98; 4.21; 4.49	2.74; 4.11; 4.53; 4.71	2.77; 3.75; 3.94; 4.01
III-100	2.65; 3.47; 3.90; 4.02	2.72; 3.81; 4.05; 4.19	2.67; 3.89; 3.99; 4.09	2.43; 3.21; 3.68; 3.89
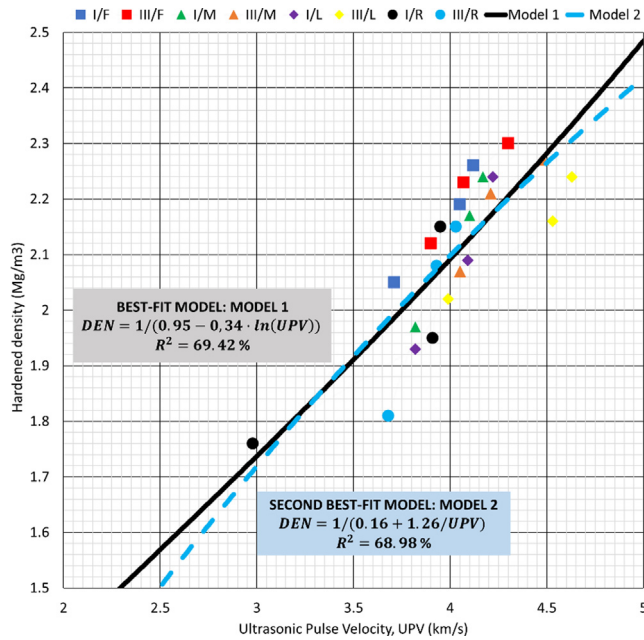
Fig. 13. Global models with better fits for the relationship between hardened density and UPV.

$$DEN = \frac{1}{0.95 - 0.34 \cdot ln(UPV)} \tag{6}$$

$$DEN = \frac{1}{0.16 + \frac{1.26}{UPV}} \tag{7}$$

3.5.2. Relationship between UPV and compressive strength

Despite the imprecise relationship between the hardened density and the UPV, the relationship obtained between this indirect measurement and compressive strength was highly accurate, as can be seen in Table 9. In this table, an analysis is shown of the relationship between compressive strength (*CS*, in MPa) and UPV

(km/s) with distinctions between modifications in the composition of the mixtures. All the developed models presented an optimum fit (coefficients R^2 greater than 97% in all cases). Nevertheless, the formulation of the models with the best fit was altered with each change in the composition of the mixes. Therefore, it is clear that the equations that establish the relationship between compressive strength and UPV are highly sensitive to the nature of the materials used in the mixture [68]. In each particular case it can be defined with high precision, although the formulation of the equation is different. This performance shows the need to evaluate different mix compositions and formulations for an accurate definition of this relationship [45], as has been done in this study. Hence, a linear equation cannot be taken as valid to describe this relationship accurately without an extensive analysis [47].

Due to the absence of a best-fit model with the same formulation in various mixtures, the development of a global model that relates compressive strength to UPV is essential, for an easy description of the relationship between these two variables. In addition, this model would have the advantages discussed above (see Section 3.4). Fig. 14 shows that it is possible to obtain a highly accurate overall model (coefficients R^2 of 97%), if a large volume of data is processed, despite the high sensitivity of the relationship between compressive strength and UPV to changes in the mix design. The two best-fit models for the relationship between these two variables are shown in Eqs. (8) and (9), respectively. These models were obtained as indicated in Section 3.4: all available data were fitted by simple regression. Once again, two models were used to avoid specific goodness-of-fit problems and to achieve greater accuracy. However, Fig. 14 also shows a problem of these global models that was not present when using the hammer rebound index: a very narrow range of UPV (3.9–4.2 km/s) is related to a very wide compressive strength interval (32–52 MPa). Hence, slight variations in the measured UPV lead to a considerable over- or underestimation of compressive strength.

$$CS = \left(-11.76 + 9.17 \cdot \sqrt{UPV}\right)^2, \quad if \quad 2.0 < UPV$$
$$< 2.7 \; and \; 4.4 < UPV < 5.0 \tag{8}$$

$$CS = (-3.22 + 2.45 \cdot UPV)^2, \quad if \quad 2.7 < UPV < 4.4 \tag{9}$$

Table 9
Compressive strength (MPa) as a function of UPV (km/s).

|		Model expression	Coefficient R^2 (%)
Mixes with the same kind of cement	Mixes with CEM I	$CS = \left(0.87 + 0.36 \cdot UPV^2\right)^2$	97.23
		$CS = (-3.41 + 2.50 \cdot UPV)^2$	97.05
	Mixes with CEM III/A	$CS = -15.69 + 3.70 \cdot UPV^2$	98.19
		$CS = \left(-11.61 + 9.10 \cdot \sqrt{UPV}\right)^2$	97.92
Mixes with the same RCA 0/4 mm content	Mixes with 0% RCA 0/4 mm	$CS = -15.23 + 3.72 · \cdot UPV^2$	97.64
		$CS = \left(-11.38 + 9.02 · \cdot \sqrt{UPV}\right)^2$	97.63
	Mixes with 50% RCA 0/4 mm	$CS = (-3.08 + 2.41 \cdot UPV)^2$	96.94
		$CS = \left(-11.53 + 9.06 \cdot \sqrt{UPV}\right)^2$	96.79
	Mixes with 100% RCA 0/4 mm	$CS = (-4.85 + 8.17 \cdot \ln(UPV))^2$	97.54
		$CS = \left(-11.57 + 9.04 \cdot \sqrt{UPV}\right)^2$	97.52
Mixes with the same aggregate powder	Mixes with limestone filler	$CS = exp(6.58 - 11.21/UPV)$	98.84
		$CS = exp(-0.77 + 3.27 \cdot \ln(UPV))$	98.73
	Mixes with limestone filler and limestone fines 0/1 mm	$CS = exp(6.68 - 11.58/UPV)$	99.03
		$CS = exp\left(-0.80 + 3.30 · \cdot \ln(UPV)\right)$	98.73
	Mixes with limestone fines 0/0.5 mm	$CS = (-2.42 + 2.25 \cdot UPV)^2$	97.03
		$CS = -13.48 + 3.57 \cdot UPV^2$	97.01
	Mixes with RCA 0/0.5 mm	$CS = (13.19 - 27.10/UPV)^2$	97.21
		$CS = (-5.10 + 8.34 \cdot \ln(UPV))^2$	97.05
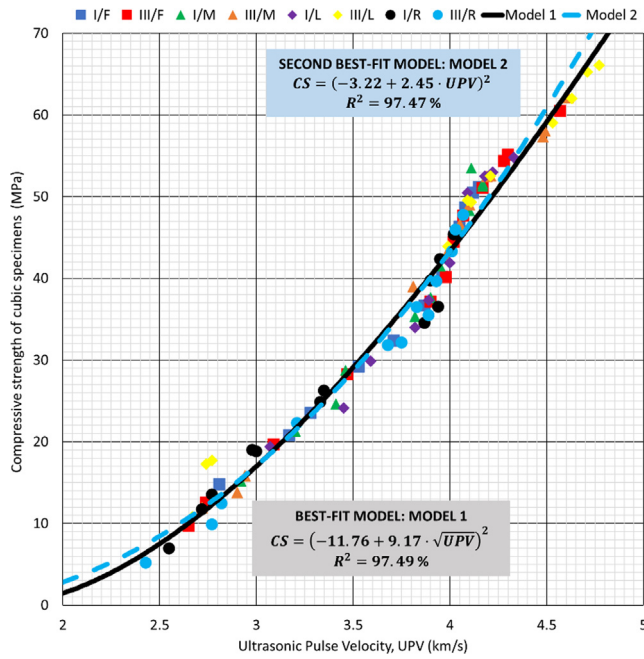
Fig. 14. Global models with the best fit for the relationship between compressive strength and UPV.
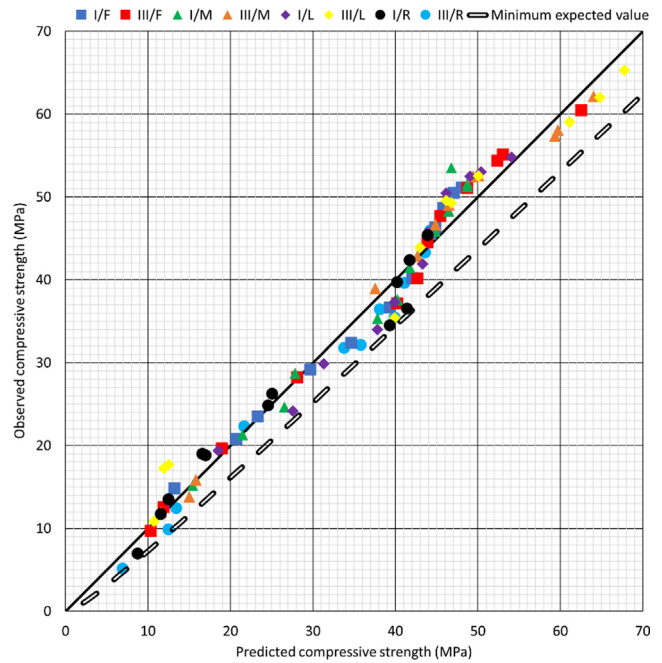

Fig. 15. Comparison between predicted compressive strength through UPV global model (Table 10) and observed compressive strength.

As in the hammer rebound index, Table 10 shows the most likely (W_m) and the least likely (W_{min}) compressive strengths of a set of cubic specimens as a function of the UPV test results. These results were obtained by the joint treatment of both models (Eqs. (8) and (9)), also shown in Fig. 14, and mean that the procedures can be homogenized, facilitating the use of these models in real works. The comparison between the observed compressive strength and the one estimated by this model is graphically represented in Fig. 15. The estimate for this indirect measure was also accurate and there was no observed strength below the minimum expected value. However, the UPV model had a wider safety interval than the hammer rebound index model, due to the different problems that have previously been discussed, mainly the high influence of the mix components, and the slight variation of the UPV value for compressive strengths between 32 and 52 MPa. It meant that the compressive strength estimation was more uncertain when UPV was used. Nevertheless, the UPV compressive-strength estimate was lower than the estimate based on the hammer rebound index, which showed that this non-destructive testing could be also used to estimate the compressive strength of concrete at early ages [20].

3.6. Joint use of the hammer rebound index and the UPV

The highly accurate models described in the previous sections, to predict compressive strength through the hammer rebound index or UPV analysis of a SF3 class SCC, mean that the composition effect of the mix may be disregarded for the prediction of SCC strength [69]. Nevertheless, the use of a single indirect measure can lead to incorrect strength estimations, due to a wide variety of reasons, from poor calibration of the device used to occasional irregularities within the concrete [2]. The best solution to this problem is to use models with two variables (hammer rebound index, and UPV) to estimate the strength, although they have the disadvantage of complexity and their implementation is difficult [1].

In this study, among the many existing functions that combine the effect of the hammer rebound index and UPV to estimate compressive strength, intuition appeared preferable to complex mathematic analyses. On the other hand, the validity of the simplest possible regression model, the linear equation, for this relationship is shown in both Table 6 and Table 9 (in Table 6, six over nine linear functions; and, in Table 9, six over nine quasi-linear functions).

Table 10
Global model for the estimation of the compressive strength on cubic specimens as a function of UPV (km/s).

UPV	W_m	W_{min}	UPV	W_m	W_{min}	UPV	W_m	W_{min}	UPV	W_m	W_{min}	UPV	W_m	W_{min}	UPV	W_m	W_{min}
2	2.1	1.0	2.55	8.7	6.2	3.05	18.1	14.4	3.55	30.2	25.4	4.05	44.9	38.9	4.55	61.8	54.8
2.05	2.6	1.3	2.60	9.5	6.9	3.10	19.2	15.4	3.60	31.6	26.6	4.10	46.5	40.4	4.60	63.7	56.5
2.10	3.0	1.6	2.65	10.4	7.6	3.15	20.3	16.4	3.65	33.0	27.9	4.15	48.1	41.9	4.65	65.5	58.2
2.15	3.5	2.0	2.70	11.2	8.3	3.20	21.5	17.4	3.70	34.4	29.2	4.20	49.7	43.5	4.70	67.4	60.0
2.20	4.0	2.4	2.75	12.1	9.1	3.25	22.6	18.5	3.75	35.8	30.5	4.25	51.4	45.0	4.75	69.3	61.7
2.25	4.6	2.8	2.80	13.0	9.9	3.30	23.8	19.6	3.80	37.2	31.9	4.30	53.1	46.6	4.80	71.2	63.5
2.30	5.2	3.3	2.85	14.0	10.8	3.35	25.1	20.7	3.85	38.7	33.2	4.35	54.8	48.2	4.85	73.1	65.3
2.35	5.9	3.8	2.90	15.0	11.6	3.40	26.3	21.8	3.90	40.2	34.6	4.40	56.5	49.8	4.90	75.0	67.2
2.40	6.5	4.4	2.95	16.0	12.5	3.45	27.6	23.0	3.95	41.7	36.0	4.45	58.3	51.4	4.95	77.0	69.0
2.45	7.2	4.9	3.00	17.0	13.4	3.50	28.9	24.2	4.00	43.3	37.5	4.50	60.0	53.1	5.00	79.0	70.9
2.50	8.0	5.5															

W_m: most likely compressive strength value (MPa)
W_{min}: minimum expected compressive strength value (MPa)

Moreover, the Pearson matrix (Fig. 16) showed a high linear correlation between both indirect measurements under study and the compressive strength. Therefore, a multiple quasi-linear regression model (Eq. (10)) with a first-power interaction term by adjusting all available data was defined to estimate compressive strength (*CS*, in MPa) through the introduction of the hammer rebound index values (*HRI*, values from 10 to 60 units) and the UPV values (from 2.5 to 5.5 km/s). This model showed a high precision, with a coefficient R^2 of 98.50%.

$$CS = -30.94 + 0.16 \cdot HRI + 12.86 \cdot UPV + 0.13 \cdot HRI \cdot UPV \quad R^2 = 98.50\% \tag{10}$$

Although this model is quite simple, Fig. 17 shows that the combination of both non-destructive testing offers a precise and safe way of estimating compressive strength. The difference between the most overestimated experimental strength and the corresponding estimated strength is not even 4 MPa, an acceptable margin for structural calculations with the conventional safety coefficients [70]. This high precision is due to the fact that the estimation errors of one indirect measurement are compensated by the other. This model clearly improves the precision of other similar models performed up to date for recycled concrete, which combine indirect measures and semi-destructive methods [44].
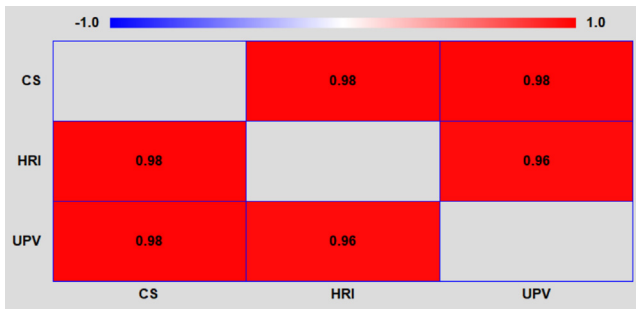

Fig. 16. Pearson product-moment correlations between hammer rebound index (HRI), the UPV, and compressive strength (CS).
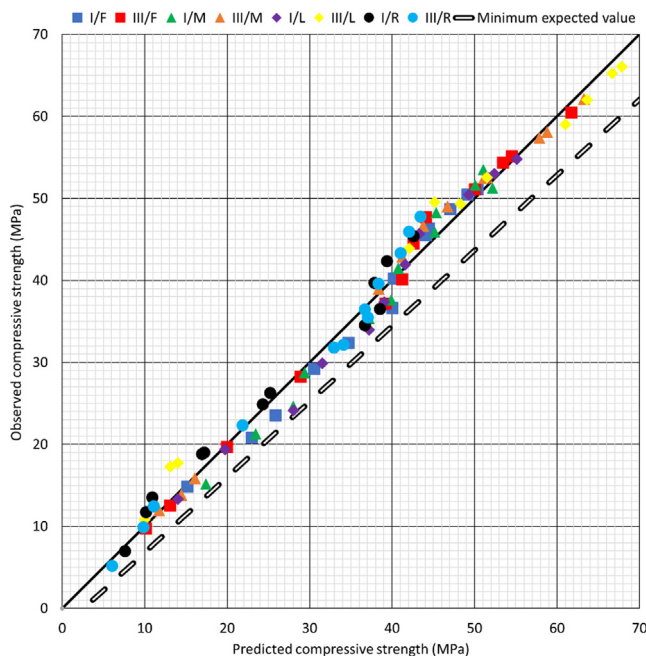
Finally, Eq. 11 yields the minimum expected value of compressive strength of this two-variable model. In this equation, *meCS* is the minimum expected compressive strength, in MPa, and *CS* is the estimated compressive strength, in MPa, calculated by Eq. (10).

$$meCS = 0.92 \cdot CS - 3.15$$

3.7. Validation of the models developed

The desirable validation of a model with data obtained from other studies is, in this case, difficult, because this is the first study in which the suitability of indirect measures has been studied in SF3 class SCC, as indicated in section 1.1. To date, this aspect has neither been analyzed in many studies on SCC of class SF2 (slump flow between 650 and 750 mm), nor there is a general model for this type of SCC. Moreover, fresh and hardened properties of SCC are very sensitive to changes in its composition [31], so any variation in its flowability could significantly affect the accuracy of the estimated compressive strength.

The global model represented in Eqs. 10 and 11 was tested with data obtained from existing research works that studied both indirect measures in SF2 class SCC [30,47,71–73]. The comparison between the observed values of the referenced studies and those calculated by the model is shown in Fig. 18. As expected, the fit of data from other studies was less accurate than the data with which the model was developed. Nevertheless, the adjustment for SF2 class SCC is considered correct, since the average deviation in absolute value of the predicted compressive strength compared to the observed one was only 5.5%.

Two aspects of the validation should be highlighted:

- Firstly, it can be seen that the compressive strength was, in most cases, underestimated by the model. This underestimate was due to the lower flowability of the SCC, generally linked to the increase in its compressive strength [41]. Thus, SF2 class SCC yielded slightly higher compressive strengths (around 2–6 MPa in the samples under study) for similar values of indirect measurements.
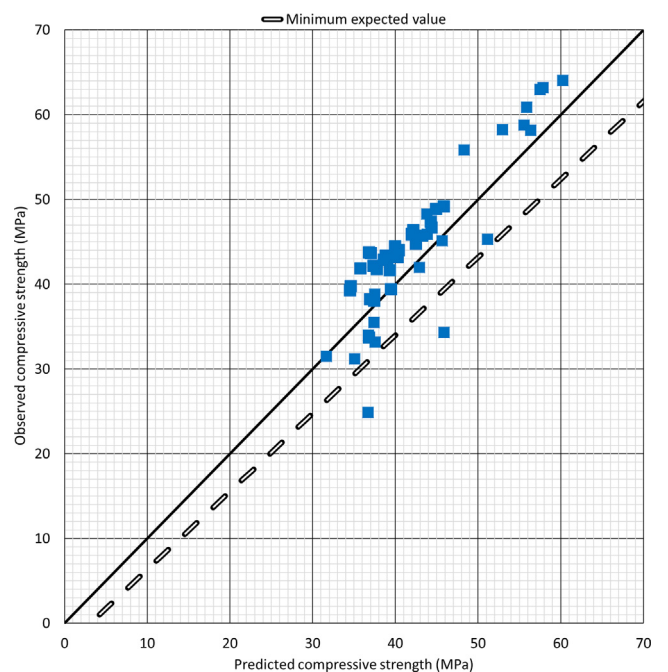

Fig. 17. Comparison between predicted compressive strength through the two-variable model and observed compressive strength.

Fig. 18. Validation of the proposed model.

- On the other hand, the cases in which the compressive strength was overestimated corresponded to SCC mixtures with a very high content of RCA and alternative binders (in particular, fly ash), which can in some cases lead to a sharp decrease in strength [58]. Nevertheless, 90% of the mixes under study were above the minimum expected value, which shows that the safety margin provided by the model is adequate.

From this study, it can be inferred that the use of the developed models in SF2 class SCC can be considered safe for medium-strength SCC mixtures with a moderate content of by-products.

3.8. Use of the models

Throughout this paper, several models for estimating the compressive strength through non-destructive testing of a highly SCC have been provided. The proposed models can be used in two different ways:

- On the one hand, the equations obtained for a particular composition of SCC (type of cement, fine RCA content, and aggregate powder nature) can be employed, which are shown in Tables 6 and 9. Each SCC mixture will usually fulfill one condition regarding each of its components, that is, six models could be used. Despite the accuracy of the models and their coefficient R^2, they can have specific goodness-of-fit problems, as explained in Section 3.4.2. The authors therefore recommend that the arithmetic mean of the results of the six equations be calculated for safe and precise estimations and to compensate for potential deviations.
- On the other hand, compressive strength can be estimated through the global models that have been developed (Table 7, Table 10, Eqs. 11 and 12). This option is recommended by the authors, because specific goodness-of-fit problems were minimized during their development, and the minimum expected values of compressive strength were calculated. In addition, these models are not dependent on the composition of the SCC. Finally, the models are easier to use: the value of the hammer rebound index and/or the UPV of the mixture is introduced in the model directly, which quickly provides both the most likely, and the minimum expected compressive strength.

4. Conclusions

In this paper, the possibility of estimating the compressive strength through the hammer rebound index and the Ultrasonic Pulse Velocity (UPV) of highly Self-Compacting Concrete (SCC) that incorporates large amounts of Recycled Concrete Aggregate (RCA) has been assessed.

A total of 24 SF3 class SCCs were developed to perform this study, with different types of cement (CEM I or CEM III/A), fine RCA contents, and types of aggregate powder. The hammer rebound index, UPV, and the compressive strength of all mixtures were determined at 1, 7, 28, and 90 days.

From the investigation, it was concluded that the mixtures manufactured with 50% fine RCA optimized flowability, and compressive strength simultaneously. Furthermore, the compressive strength could be increased by the addition of CEM III/A, with around 45% of GGBFS, due to the necessary replacement of coarse aggregate by binder that was performed in these mixes to achieve SF3 class SCC. This change also led the surface hardness of these mixtures to depend more on the added binder, which produced higher increases in the hammer rebound index than in conventional concretes. On the other hand, the use of this alternative binder delayed the development of strength over time, which meant that the UPV values were not proportionate to the rise in compres-sive strength at advanced ages. Finally, the joint use of fine RCA and CEM III/A also yielded suitable in-fresh and hardened behaviors.

On the other hand, indirect, accurate, and safe estimation of the compressive strength of highly SCC, regardless of the mix composition, has been developed and verified with the data from other studies. High precision models were obtained (Table 7, Table 10, Eqs. 11 and 12).

From the aspects discussed throughout this article, the main conclusions drawn are:

- The existing models for estimating the compressive strength in non-recycled vibrated concrete through non-destructive testing were not valid for SF3 class SCC. The hammer rebound index underestimated the strength, while the use of the UPV test led to an overestimation. These discrepancies were attributed to the high content of the fine aggregate fractions that were required to achieve such high levels of flowability.
- The model designed in this study to estimate compressive strength as a function of the hammer rebound index presented a robust formulation that was not affected by variations in the composition of the mixtures, except for the nature of the aggregate powder. The relationship between the compressive strength and the UPV was much more sensitive, as it was affected by any minimal change of the materials used in the mix.
- The safety interval provided by the UPV model designed in this study was slightly higher than when the hammer rebound index was used to estimate compressive strength. This result indicates that the prediction of compressive strength of SF3 class SCCs using the UPV model has a higher uncertainty, and small changes to the value of this indirect measure can imply large differences in the estimated strength.
- The estimation of compressive strength from one single indirect measurement, the hammer rebound or the UPV, yielded robust predictions. However, the combined use of both, by means of a simple quasi-linear equation, yielded estimations of greater precision.

In short, this study has provided robust models for predicting the compressive strength through indirect measurements (hammer rebound index or/and UPV) for SF3 class SCCs. These models promote the use of recycled concretes in real structures, by providing a tool with which to monitor their strength during their construction and lifecycle through non-destructive testing. Moreover, the models and procedures explained in this article can be used as a basis for the development of similar models for other recycled and/or non-conventional types of concrete. This study has, therefore, opened up a very interesting future line of research.

Declaration of Competing Interest

The authors declare that they have no known competing financial interests or personal relationships that could have appeared to influence the work reported in this paper.

Acknowledgements

References

[1] R. Jones, The non-destructive testing of concrete, Mag. Concr. Res. 1 (2) (1949) 67–78, https://doi.org/10.1680/macr.1949.1.2.67.

[2] A. Aseem, W. Latif Baloch, R.A. Khushnood, A. Mushtaq, Structural health assessment of fire damaged building using non-destructive testing and micrographical forensic analysis: a case study, Case Stud, Constr. Mater. 11 (2019) e00258, https://doi.org/10.1016/j.cscm.2019.e00258.

[3] U. Dolinar, G. Trtnik, G. Turk, T. Hozjan, The feasibility of estimation of mechanical properties of limestone concrete after fire using nondestructive methods, Constr. Build. Mater. 228 (2019) 116786, https://doi.org/10.1016/j.conbuildmat.2019.116786.

[4] G.W. Greene, Test hammer provides new method of evaluating hardened concrete, ACI J. Proc. 51 (11) (1954) 249–256.

[5] R. Jones, The ultrasonic testing of concrete, Ultrasonics 1 (2) (1963) 78–82, https://doi.org/10.1016/0041-624X(63)90058-1.

[6] K.C. Hover, Case studies of non-destructive test results and core strengths at age of 3-days, Constr. Build. Mater. 227 (2019) 116672, https://doi.org/10.1016/j.conbuildmat.2019.116672.

[7] H. Qasrawi, Effect of the position of core on the strength of concrete of columns in existing structures, J. Build. Eng. 25 (2019) 100812, https://doi.org/10.1016/j.jobe.2019.100812.

[8] J.H. Bungey, S.G. Millard, M.G. Grantham, Testing of Concrete in Structures, London: Taylor & Francis, 2006 p. 352. (2006).

[9] ACI-228.1R-19, In-place methods to estimate concrete strength (2019).

[10] D.J. Victor, Evaluation of hardened field concrete with rebound hammer, ACI Mater. J. 37 (11) (1963) 407–411.

[11] J. Kolek, An appreciation of the Schmidt rebound hammer, Mag. Concr. Res. 10 (28) (1958) 27–36, https://doi.org/10.1680/macr.1958.10.28.27.

[12] W.E. Grieb, Use of Swiss hammer for establishing the compressive strength of hardened concrete, Public Roads 201 (1958) 1–14.

[13] K. Wesche, Possibilities for the application of ultrasounds in concrete testing, Bautechnik 32 (1955) 151–155.

[14] S. Popovics, J.S. Popovics, Critique of the ultrasonic pulse velocity method for testing concrete, Proceedings of Nondestructive Testing of Concrete Elements and Structures, Publ by ASCE, New York, NY, United States San Antonio, TX, USA, 1992, pp. 94-103.

[15] ASTM-C597-16, Standard test method for pulse velocity through concrete (2016).

[16] S.F. Selleck, E.N. Landis, M.L. Peterson, S.P. Shah, J.D. Achenbach, Ultrasonic investigation of concrete with distributed damage, ACI Mater. J. 95 (1) (1998) 27–36.

[17] W. Punurai, J. Jarzynski, J. Qu, K.E. Kurtis, L.J. Jacobs, Characterization of entrained air voids in cement paste with scattered ultrasound, NDT E. Int. 39 (6) (2006) 514–524, https://doi.org/10.1016/j.ndteint.2006.02.001.

[18] J.R. Leslie, W.J. Cheesman, An ultrasonic method of studying deterioration and cracking in concrete structure, J. Am. Concr. Inst. 46 (1949) 17–36.

[19] G. Barluenga, J. Puentes, I. Palomar, C. Guardia, Methodology for monitoring Cement Based Materials at Early Age combining NDT techniques, Constr. Build. Mater. 193 (2018) 373–383, https://doi.org/10.1016/j.conbuildmat.2018.10.205.

[20] M. Benaicha, O. Jalbaud, X. Roguiez, A. Hafidi Alaoui, Y. Burtschell, Prediction of Self-Compacting Concrete homogeneity by ultrasonic velocity, Alexandria Eng. J. 54 (4) (2015) 1181–1191, https://doi.org/10.1016/j.aej.2015.08.002.

[21] R. Latif Al-Mufti, A.N. Fried, The early age non-destructive testing of concrete made with recycled concrete aggregate, Constr. Build. Mater. 37 (2012) 379–386, https://doi.org/10.1016/j.conbuildmat.2012.07.058.

[22] N.T. Nguyen, Z.-M. Sbartaï, J.-F. Lataste, D. Breysse, F. Bos, Assessing the spatial variability of concrete structures using NDT techniques – laboratory tests and case study, Constr. Build. Mater. 49 (2013) 240–250, https://doi.org/10.1016/j.conbuildmat.2013.08.011.

[23] A.M. Ley-Hernandez, D. Feys, J.A. Hartell, Effect of dynamic segregation of self-consolidating concrete on homogeneity of long pre-cast beams, Mater. Struct. 52 (1) (2019) 4, https://doi.org/10.1617/s11527-018-1303-z.

[24] T. Xu, J. Li, Assessing the spatial variability of the concrete by the rebound hammer test and compression test of drilled cores, Constr. Build. Mater. 188 (2018) 820–832, https://doi.org/10.1016/j.conbuildmat.2018.08.138.

[25] Y. Boukari, D. Bulteel, P. Rivard, N.E. Abriak, Combining nonlinear acoustics and physico-chemical analysis of aggregates to improve alkali-silica reaction monitoring, Cem. Concr. Res. 67 (2015) 44–51, https://doi.org/10.1016/j.cemconres.2014.08.005.

[26] H. Sasanipour, F. Aslani, Effect of specimen shape, silica fume, and curing age on durability properties of self-compacting concrete incorporating coarse recycled concrete aggregates, Constr. Build. Mater. 228 (2019) 117054, https://doi.org/10.1016/j.conbuildmat.2019.117054.

[27] G. Washer, P. Fuchs, B.A. Graybeal, J.L. Hartmann, Ultrasonic testing of reactive powder concrete, IEEE Trans. Ultrason. Ferroelectr. Freq. Control 51 (2) (2004) 193–201, https://doi.org/10.1109/TUFFC.2004.1320767.

[28] P.N. Hiremath, S.C. Yaragal, Performance evaluation of reactive powder concrete with polypropylene fibers at elevated temperatures, Constr. Build. Mater. 169 (2018) 499–512, https://doi.org/10.1016/j.conbuildmat.2018.03.020.

[29] M. Benaicha, O. Jalbaud, A. Hafidi Alaoui, Y. Burtschell, Correlation between the mechanical behavior and the ultrasonic velocity of fiber-reinforced concrete,

Constr. Build. Mater. 101 (2015) 702–709, https://doi.org/10.1016/j.conbuildmat.2015.10.047.

[30] M.C.S. Nepomuceno, L.F.A. Bernardo, Evaluation of self-compacting concrete strength with non-destructive tests for concrete structures, Appl. Sci. 9 (23) (2019) 5109, https://doi.org/10.3390/app9235109.

[31] S. Santos, P.R. da Silva, J. de Brito, Self-compacting concrete with recycled aggregates – a literature review, J. Build. Eng. 22 (2019) 349–371, https://doi.org/10.1016/j.jobe.2019.01.001.

[32] A. Santamaría, J.J. González, M.M. Losáñez, M. Skaf, V. Ortega-López, The design of self-compacting structural mortar containing steelmaking slags as aggregate, Cem. Concr. Compos. 111 (2020) 103627, https://doi.org/10.1016/j.cemconcomp.2020.103627.

[33] S.A. Santos, P.R. da Silva, J. de Brito, Mechanical performance evaluation of self-compacting concrete with fine and coarse recycled aggregates from the precast industry, Mater. 10 (8) (2017) 904, https://doi.org/10.3390/ma10080904.

[34] A. Singh, Z. Duan, J. Xiao, Q. Liu, Incorporating recycled aggregates in self-compacting concrete: a review, J. Sustain. Cem. Based Mater. 9 (3) (2020) 165–189, https://doi.org/10.1080/21650373.2019.1706205.

[35] F. Debieb, S. Kenai, The use of coarse and fine crushed bricks as aggregate in concrete, Constr. Build. Mater. 22 (5) (2008) 886–893, https://doi.org/10.1016/j.conbuildmat.2006.12.013.

[36] C. Pellegrino, F. Faleschini, Experimental behavior of reinforced concrete beams with electric arc furnace slag as recycled aggregate, ACI Mater. J. 110 (2) (2013) 197–205.

[37] M. Etxeberria, A. Gonzalez-Corominas, The assessment of ceramic and mixed recycled aggregates for high strength and low shrinkage concretes, Mater. Struct. 51 (5) (2018) 129, https://doi.org/10.1617/s11527-018-1244-6.

[38] A.R. Khan, S. Fareed, M.S. Khan, Use of recycled concrete aggregates in structural concrete, Sustain. Constr. Mater. Technol. 2 (2019).

[39] D. Pedro, J. de Brito, L. Evangelista, Durability performance of high-performance concrete made with recycled aggregates, fly ash and densified silica fume, Cem. Concr. Compos. 93 (2018) 63–74, https://doi.org/10.1016/j.cemconcomp.2018.07.002.

[40] C. Shi, Y. Li, J. Zhang, W. Li, L. Chong, Z. Xie, Performance enhancement of recycled concrete aggregate - a review, J. Clean. Prod. 112 (2016) 466–472, https://doi.org/10.1016/j.jclepro.2015.08.057.

[41] F. Fiol, C. Thomas, C. Muñoz, V. Ortega-López, J.M. Manso, The influence of recycled aggregates from precast elements on the mechanical properties of structural self-compacting concrete, Constr. Build. Mater. 182 (2018) 309–323, https://doi.org/10.1016/j.conbuildmat.2018.06.132.

[42] H.S. Gökçe, O. Şimşek, The effects of waste concrete properties on recycled aggregate concrete properties, Mag. Concr. Res. 65 (14) (2013) 844–854, https://doi.org/10.1680/macr.12.00181.

[43] B.B. Mukharjee, S.V. Barai, Influence of Nano-Silica on the properties of recycled aggregate concrete, Constr. Build. Mater. 55 (2014) 29–37, https://doi.org/10.1016/j.conbuildmat.2014.01.003.

[44] M. Kazemi, R. Madandoust, J. de Brito, Compressive strength assessment of recycled aggregate concrete using Schmidt rebound hammer and core testing, Constr. Build. Mater. 224 (2019) 630–638, https://doi.org/10.1016/j.conbuildmat.2019.07.110.

[45] V. Revilla-Cuesta, M. Skaf, F. Faleschini, J.M. Manso, V. Ortega-López, Self-compacting concrete manufactured with recycled concrete aggregate: an overview, J. Clean. Prod. 262 (2020) 121362, https://doi.org/10.1016/j.jclepro.2020.121362.

[46] R. Sri Ravindrajah, Y.H. Loo, C.T. Tam, Strength evaluation of recycled-aggregate concrete by in-situ tests, Mater. Struct. 21 (4) (1988) 289–295, https://doi.org/10.1007/BF02481828.

[47] N. Singh, S.P. Singh, Evaluating the performance of self compacting concretes made with recycled coarse and fine aggregates using non destructive testing techniques, Constr. Build. Mater. 181 (2018) 73–84, https://doi.org/10.1016/j.conbuildmat.2018.06.039.

[48] P. Kumar, N. Singh, Influence of recycled concrete aggregates and Coal Bottom Ash on various properties of high volume fly ash-self compacting concrete, J. Build. Eng. 32 (2020) 101491, https://doi.org/10.1016/j.jobe.2020.101491.

[49] EFNARC, Specification Guidelines for Self-compacting Concrete, European Federation of National Associations Representing producers and applicators of specialist building products for Concrete (2002).

[50] F. Van Der Vurst, S. Grünewald, D. Feys, K. Lesage, L. Vandewalle, J. Vantomme, G. De Schutter, Effect of the mix design on the robustness of fresh self-compacting concrete, Cem. Concr. Compos. 82 (2017) 190–201, https://doi.org/10.1016/j.cemconcomp.2017.06.005.

[51] EN-Euronorm, Rue de stassart, 36. Belgium-1050 Brussels, European Committee for Standardization (2020).

[52] I. González-Taboada, B. González-Fonteboa, J. Eiras-López, G. Rojo-López, Tools for the study of self-compacting recycled concrete fresh behaviour: workability and rheology, J. Clean. Prod. 156 (2017) 1–18, https://doi.org/10.1016/j.jclepro.2017.04.045.

[53] E. Güneyisi, M. Gesoğlu, Z. Algin, H. Yazici, Effect of surface treatment methods on the properties of self-compacting concrete with recycled aggregates, Constr. Build. Mater. 64 (2014) 172–183, https://doi.org/10.1016/j.conbuildmat.2014.04.090.

[54] D. Carro-López, B. González-Fonteboa, J. De Brito, F. Martínez-Abella, I. González-Taboada, P. Silva, Study of the rheology of self-compacting concrete with fine recycled concrete aggregates, Constr. Build. Mater. 96 (2015) 491-501. 7102. DOI:10.1016/j.conbuildmat.2015.08.091.

[55] Proceq, Sclerometer types N and NR: instructions for use (2020).

[56] I. Facadaru, Non-destructive testing of concrete in Romania, Non-Destructive Test. 2 (1) (1969) 48, https://doi.org/10.1016/0029-1021(69)90085-1.

[57] H. Okamura, M. Ouchi, Self-compacting concrete, J. Adv. Concr. Technol. 1 (1) (2003) 5–15, https://doi.org/10.3151/jact.1.5.

[58] C. Sun, Q. Chen, J. Xiao, W. Liu, Utilization of waste concrete recycling materials in self-compacting concrete, Resour. Conserv. Recycl. 161 (2020) 104930, https://doi.org/10.1016/j.resconrec.2020.104930.

[59] H. Salehi, M. Mazloom, Opposite effects of ground granulated blast-furnace slag and silica fume on the fracture behavior of self-compacting lightweight concrete, Constr. Build. Mater. 222 (2019) 622–632, https://doi.org/10.1016/j.conbuildmat.2019.06.183.

[60] I. González-Taboada, B. González-Fonteboa, F. Martínez-Abella, S. Seara-Paz, Analysis of rheological behaviour of self-compacting concrete made with recycled aggregates, Constr. Build. Mater. 157 (2017) 18–25, https://doi.org/10.1016/j.conbuildmat.2017.09.076.

[61] T.A. Rebello, R. Zulcão, J.L. Calmon, R.F. Gonçalves, Comparative life cycle assessment of ornamental stone processing waste recycling, sand, clay and limestone filler, Waste Manage. Res. 37 (2) (2019) 186–195, https://doi.org/10.1177/0734242X18819976.

[62] Z. Duan, A. Singh, J. Xiao, S. Hou, Combined use of recycled powder and recycled coarse aggregate derived from construction and demolition waste in self-compacting concrete, Constr. Build. Mater. 254 (2020) 119323, https://doi.org/10.1016/j.conbuildmat.2020.119323.

[63] O.K. Djelloul, B. Menadi, G. Wardeh, S. Kenai, Performance of self-compacting concrete made with coarse and fine recycled concrete aggregates and ground granulated blast-furnace slag, Adv. Concr. Constr. 6 (2) (2018) 103–121, https://doi.org/10.12989/acc.2018.6.2.103.

[64] W.C. Jau, C.T. Yang, Development of a modified concrete rheometer to measure the rheological behavior of conventional and self-consolidating concretes, Cem. Concr. Compos. 32 (6) (2010) 450–460, https://doi.org/10.1016/j.cemconcomp.2010.01.001.

[65] S.C. Kou, C.S. Poon, Properties of self-compacting concrete prepared with coarse and fine recycled concrete aggregates, Cem. Concr. Compos. 31 (9) (2009) 622–627, https://doi.org/10.1016/j.cemconcomp.2009.06.005.

[66] A. Santamaría, V. Ortega-López, M. Skaf, J.A. Chica, J.M. Manso, The study of properties and behavior of self compacting concrete containing Electric Arc Furnace Slag (EAFS) as aggregate, Ain Shams Eng. J. 11 (1) (2020) 231–243, https://doi.org/10.1016/j.asej.2019.10.001.

[67] R. Feiz, J. Ammenberg, L. Baas, M. Eklund, A. Helgstrand, R. Marshall, Improving the CO2 performance of cement, part I: utilizing life-cycle assessment and key performance indicators to assess development within the cement industry, J. Clean. Prod. 98 (2015) 272–281, https://doi.org/10.1016/j.jclepro.2014.01.083.

[68] D. Breysse, X. Romão, M. Alwash, Z.M. Sbartaï, V.A.M. Luprano, Risk evaluation on concrete strength assessment with NDT technique and conditional coring approach, J. Build. Eng. 32 (2020) 101541, https://doi.org/10.1016/j.jobe.2020.101541.

[69] F. Moutassem, S.E. Chidiac, Assessment of concrete compressive strength prediction models, KSCE J. Civ. Eng. 20 (1) (2016) 343–358, https://doi.org/10.1007/s12205-015-0722-4.

[70] A.S. Brand, A.N. Amirkhanian, J.R. Roesler, Flexural capacity of full-depth and two-lift concrete slabs with recycled aggregates, Transp. Res. Rec. 2456 (1) (2014) 64–72, https://doi.org/10.3141/2456-07.

[71] C.K. Mahapatra, S.V. Barai, Sustainable self compacting hybrid fiber reinforced concrete using waste materials, Struct. Concr. 20 (2) (2019) 756–765, https://doi.org/10.1002/suco.201700239.

[72] V. Revilla-Cuesta, V. Ortega-López, M. Skaf, J.M. Manso, Effect of fine recycled concrete aggregate on the mechanical behavior of self-compacting concrete, Constr. Build. Mater. 263 (2020) 120671, https://doi.org/10.1016/j.conbuildmat.2020.120671.

[73] L. Rojas-Henao, J. Fernández-Gómez, J.C. López-Agüí, Rebound hammer, pulse velocity, and core tests in self-consolidating concrete, ACI Mater. J. 109 (2) (2012) 235–243.